A Doctoral Dissertation

Development of high-performance spongiform adsorbents with caged Prussian blue as the absorbing elements for radioactive cesium decontamination

プルシアンブルーを内包した放射性セシウムを除染するための高性能スポンジ型吸着材の開発

Baiyang Hu

北海道大学
HOKKAIDO UNIVERSITY

Division of Environmental Science Development,

Graduate School of Environmental Science,

Hokkaido University,

Sapporo, Japan (2014)

Contents

Abstract

High-performance spongiform adsorbents with Prussian blue particles being caged into the cell-walls have been developed for the decontamination of radioactive cesium. Radioactive cesium has been introduced into our environment since the nuclear weapon testing during the 1950s and 1960s and the nuclear power plants accidents in recent years such as Chernobyl and Fukushima disaster. Concerns associated with radioactive cesium are main focusing on the long half-life species (Cesium-137, $T_{1/2}$=30 years; Cesium-134, $T_{1/2}$=2.06 years) and thereby the strong gamma radiation emission, their high solubility and the high potential mobility in environment, their high selectivity toward the biological systems due to the metabolic similarity with potassium and the cause of thyroid cancer. Hence, the elimination of radioactive cesium from a certain contaminated environment is one of the most important tasks towards achieving the goal of environmental remediation. Prussian blue (Ferric hexacyanoferrate) has long been considered as a powerful absorbing element for elimination of radioactive cesium due to its unique adsorption selectivity and the high capacity. However, due to its intrinsic property of forming a colloid in water, small

sized Prussian blue particles can easily contaminate water; thus, practical applications have long been limited to the medical and/or pharmaceutical treatments.

In this study, we have developed a caging approach to overcome the intrinsic difficulties associated with colloidal dispersion of Prussian blue in water to create high-performance spongiform adsorbents for eliminating the radioactive cesium from low level radioactive water.

This thesis paper is composing of 4 chapters. In Chapter 1, a brief introduction to the detrimental impacts of radioactive cesium to our environment and the use of Prussian blue as a potential adsorbent for cesium decontamination as well as the difficulties encountered in the practical elimination applications were described. In Chapter 2, the caging of Prussian blue into the cavities of diatomite adopt an *in situ* micro-packing approach was introduced. Non-toxic, low-cost and the naturally occurred abundance with cylindrical shapes as well as the ultra-high porous structures of diatomite was used as a micro-meter sized container for storage of the in situ synthesized Prussian blue particles. We have demonstrated experimentally that Prussian blue particles could be produced with certain quantities in the

cavity of diatomite through an in situ Prussian blue formation approach. An additional nano-sized network which consisted of highly-dispersed carbon nanotubes (CNTs) was created over the surface of the diatomite; this CNTs-network has firmly sealed the Prussian blue particles inside the diatomite cavities. CNTs, once being dispersed into individual tubes, have shown high tendencies to form self-assembling interconnected networks; with the CNTs-network, Prussian blue particles have been prevented from the possible diffusion from the diatomite cavities. Moreover, the CNTs-network have provided more contacting areas for the distribution of cesium and thereby enhancing water uptake into the absorbing element, namely, the caged Prussian blue. In Chapter 3, fabrication of the spongiform adsorbents with the CNTs-network/diatomite/Prussian blue as the functioning elements and the studies on the adsorptive behaviors were described. The resultant ternary (CNTs-network/diatomite/Prussian blue) composites were mixed with polyurethane pre-polymers to produce the spongiform adsorbents through an in situ foaming procedure. The CNTs-network/diatomite/Prussian blue composites have been permanently immobilized into the cell-walls of the polyurethane foam. Macro-sized, durable, and flexible spongiform adsorbents

were established. Cesium-133 was used for studying the adsorptive capabilities of the Prussian-blue based spongiform absorbent and the caged Prussian blue showed a theoretical capacity of 167mg/g for cesium, indicating a fact that the Prussian blue based spongiform is an excellent adsorbent for the adsorbent of cesium. Adsorption isotherms plotted based on Langmuir equation gave liner line, suggesting that the caged Prussian blue adsorbed cesium in the Langmuir adsorption manner. Cesium was absorbed primarily by ion-exchange mechanism. For evaluating the practical application of our spongiform adsorbent, deionized water and seawater, each containing 1.50 Bq cesium-137 were decontaminated with the spongiform adsorbent. The elimination efficiency was found to be 99.93% for the deionized water sample and 99.47% for the seawater sample, respectively; indicating the high selectivity and the high capacity for the adsorption of radioactive cesium-137. In addition, it is worth to mention that the cesium elimination with our spongiform adsorbent was accomplished by self-uptake of the radioactive species from the aqueous solution. In Chapter 4, general conclusions and the future perspective regarding the advantageous properties and the potential

application of the spongiform adsorbent for radioactive cesium decontamination were drafted.

In conclusion, in this study we have demonstrated that the radioactive cesium could be selectively eliminated from the low level radioactive water samples by using Prussian blue being caged in triplicate in spongy as the adsorbents. It is important to note here that another advantage of our spongiform adsorbents was that, after the radioactive cesium being absorbed, the adsorbent can be condensed into very small volumes through carbonization treatment. This provides a desirable yet practical strategy for reducing the final volumes of radioactive waste. All these achievements obtained in this study are highly beneficial to environmental remediation.

List of acronyms

PB	Prussian blue
CNTs	carbon nanotubes
DM	diatomite
PUP	polyurethane prepolymer
PUF	polyurethane form
SEM	scanning electron microscopy
TG-A	thermogravimetric analysis
UV-vis	Ultraviolet-visible
XRD	**X**-ray diffraction
FT-IR	fourier transform infrared spectroscopy
ICP	inductively coupled plasma,

List of figures

adsorption. Each 10.0 ml of deionized water (DW) or seawater (SW) contained cesium-137 (initial radioactivity, 1.50 Bq/ml) sample was taken up (absorbed) with 250 mg of PUF/CNTs/DM/PB, PUF/DM/PB, or the polyurethane polymer combined with diatomite (PUF/DM). *The elimination efficiency was calculated from the initial (C_0) and final (C) cesium-137 concentrations: $(C_0-C)/C_0*100\%$----------92

Chapter I

General introduction

1.1 Research background

1.1.1 Pollution of radioactive cesium

Thousands of tons of water have been catastrophically contaminated with radioactive cesium-137 after the 9.0 magnitude earthquake, followed by the tsunami on March 11, 2011 in Japan. In fact, after the earthquake and tsunami, problems on the cooling systems of the Fukushima Daiichi 1, Fukushima Daiichi 2, and Fukushima Daiichi 3 in power, all boiling water reactors (BWR), BWR were shut down automatically (Manolopoulou, Stoulos, Ioannidou, Vagena, and Papastefanou, 2013). Over 10,000 tons of low-level radioactive water had been dumped from the storage tanks into the ocean to address the more critical task of decontaminating high-level radioactive water (G.Brumfiel., 2011). According to U.S. Environmental Protection Agency (EPA), the regulatory term low-level radioactive waste (LLRW) is defined as the broad group or 'class' of radioactive waste that is not included in the following classes of radioactive waste: spent nuclear fuel, high-level waste, transuranic waste, and uranium and thorium mill tailings. Moreover, there is no limit on the amount of radioactive material that can be contained in 'low-level' radioactive waste. While, for the high-level radioactive waste, it

was described as: resulting from the reprocessing of spent nuclear fuel, and other highly radioactive material that the Commission, consistent with existing law, determines by rule requires permanent isolation.

In fact, radioactive cesium has been released into our environment since the domestic and foreign nuclear weapon testing during 1950s and 1960s and other radiological events and the nuclear power plants accidents in recently years such as Chernobyl and Fukushima disaster (C.E. Miller, 1956; Sawidis, Heinrich, and Brown, 2003). Due to a reactor accident for Chernobyl in the former Soviet Union, millions gallons of high-level radioactive wastes were stored into more than 100 steel tanks underground, however, some of these tanks are known to have leaked, and the waste is still waiting for final disposition. (Steefel, Carroll, Zhao, and Roberts, 2003). A great deal of attentions had been focused on the treatment and volume reduction of the aqueous radioactive waste as released of the radioactive cesium into the environment cause serious environmental problems as well as human health hazard. Moreover; radioactive cesium can enter the environment as a result of sabotage of terrorism. (Volchek, Miah, Kuang, DeMaleki, and Tezel, 2011)

After the Chernobyl accident in 1986, many studies on the decontamination of radioactive cesium were carried out. More than a decade after deposition on Chernobyl fallout, radioactive pollution is still localized (Yoshida, Muramatsu, Dvornik, Zhuchenko, and Linkov, 2004). Therefore, contamination of radioactive cesium is still a major concern within global society. Despite huge efforts towards safe storage of radioactive waste, we have been facing of uncontrolled release of radioactive cesium to the natural environment. Since the big nuclear accident at Fukushima, Japan in 2011, a large amount of radionuclides were released into water, soil and air, and the hazardous influence of radioactive wastewater has drawn much attention all over the world. As a result, numerous efforts have been undertaken to find effective and low cost methods to separate and remove cesium (Cs) from waste solutions (Ding, Zhao, Yang, Shi, Zhang, Lei, and Yang, 2013). Fukushima Daiichi nuclear power stations are equipped with systems constructed with zeolite as the absorbing material, and these are under maximum operation for eliminating radioactive elements from high-level radioactive water . However, currently, there are no systems capable of eliminating radioactive elements from low-level radioactive water.

1.1.2 Detrimental impacts of radioactive cesium

Cesium (chemical symbol Cs) is present in pollucite, epidolytes, granite-like bedrock and chalky deposits in vast quantities in the crust of earth (Pinsky, and Bose, 1984). There are 11 major radioactive cesium isotopes; among them, Cs-137, one of the major radioactive isotopes, formed as a by-product of processing of uranium fuels, is a major component of high level nuclear wastes around the world. However; at the same time, radioactive cesium is also very useful in industry for its strong radioactivity. For instance, radioactive cesium was used in industries to detect liquid flow in pipes and thanks, besides; thousands of devices use radioactive cesium-137.

Concerns associated with radioactive cesium are main focusing on: moderately long half-life species (Cesium-137, $T_{1/2}$=30 years; Cesium-134, $T_{1/2}$=2.06 years) and thereby strong gamma-emitting radiation. Cesium-134, cesium-135 and cesium-137 are the three isotopes that have half-lives long enough to warrant concerned. Emitting a beta particle is the feature of these decays. All of this decay by emitting beta particles with the resultant decay products emitting gamma radiation. Take radioactive cesium-137 for example, Cesium-137 decay by bate emission to a metastable nuclear isomer of

barium-137, 153 seconds is the half-life of Ba-137 and it is responsible for all of the emissions of gamma rays (Laboratory, 2005). Hence, Cesium-137 remains one of the most problematic of the radionuclides in terms of radioactive waste. The half-live of the other cesium isotopes are less than two weeks. Besides, they can be easily incorporated in terrestrial and aquatic organisms because of their chemical similarity to potassium. Therefore radioactive cesium should be removed and safely stored (Sukwarotwat, 2010).

High solubility and high potential mobility of cesium in the marine environment together with their high selectivity toward the biological systems were still concerned. It had reported that no more than 20 degree, the solubility of CsCl, $CsHCO_3$, Cs_2CO_3, and CsOH, were up to 186, 209, 261, and 400g/100g of water, respectively. Cesium is an alkali element and many of its chemical properties are similar to those of potassium (Bystrzejewska-Piotrowska, and Bazała, 2008). This character results the high potential mobility in the marine environment, as cesium can travel in airborne dust particles, and can be present in food and water. Their high selectivity toward the biological system was due to the metabolic similarity with potassium and causes of the thyroid cancer. According to the previous reports,

cesium is 100% absorbed from the gut to the body and is distributed fairly uniformly throughout the body's soft tissues. Moreover Cs-137 is the major cause of Thyroid Cancer in Belarus, which took 70% of the fallout from the Chernobyl Nuclear Disaster (Sangvanich, Sukwarotwat, Wiacek, Grudzien, Fryxell, Addleman, Timchalk, and Yantasee, 2010). As we breathe and drink, the fallout in air and water are brought directly into our bodies. Once in our body, they will continue to emit radiation directly to living tissue due to they may lodge in our lungs or digestive tract

In a word, contamination of water by radioactive cesium is a global problem as radioactive cesium ion is a significant component of nuclear waste and nuclear fallout, and elimination of radioactive cesium from a certain contaminated environment is one of the most important tasks towards the goal of environmental remediation.

1.2 Difficulties encountered in the practical elimination applications

The treatment of radioactive cesium had been studied in the past decades; ion exchange, adsorption and precipitation are the traditional methods (Zhang, Gu, Zhao, Zhang, and Deng, 2009). Although it is still a subject of debate, bioremediation might be regarded as an alternative solution for

decontamination of cesium radioisotopes (Bystrzejewska-Piotrowska et al., 2008). In a word, concentration of the radionuclides in small volumes of solid wastes is the purpose (Cortes-Martinez, Olguin, and Solache-Rios, 2010). Among these methods, adsorption is the most widely used method, due to the ease of operation; high efficiency as well as stabilities, easy handling, and comparable low cost. The adsorbent has been deemed to the most widely used material for elimination of radioactive cesium from wastewater. Various adsorbents, such as resin, natural and synthetic zeolites have been used as their ion exchange properties with cesium for a long history. Low costs and theoretical high capacities are the advantages of the zeolites. However, the efficiency was limited by the PH range; and the co-existing ions, consequently, these aspects prevent the practical application of zeolite (Rogers, Bowers, and Gates-Anderson, 2012).

Three major difficulties have been encountered in treating radioactive water; especially for the low-level radioactive water. First, the radioactive elements are extremely low in concentration (compared to co-existing abundant ions, sodium and potassium); thus, the adsorbing materials must be highly selective for the targeted radioactive species. Second, the volume of

low-level radioactive water is extremely large; thus, the treatment systems must be able to operate without pumping all the water through the entire treating system. Third, low-level radioactive water is found in distant locations; thus, treatment systems must be portable and easy to operate.

1.3 Prussian blue as a powerful absorbing element for radioactive cesium

Adsorption has been considered as an effective method for the decontaminant of radioactive elements in environment. Prussian blue (PB)

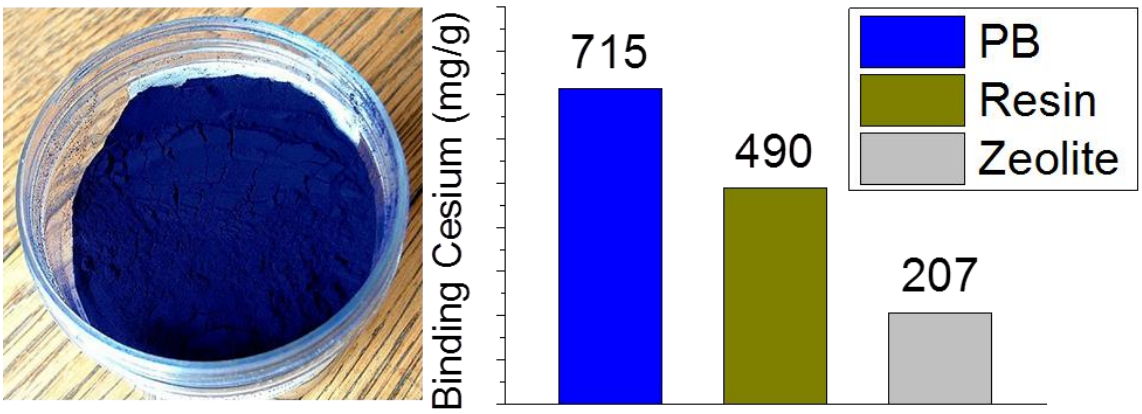

Figure 1-1 Powders of Prussian blue particles (left) and a survey on the publications with cesium binding capability for different adsorbents (right)

or iron (III) hexacyanoferrate (II), one of the first, man-made coordination compounds, widely known as “the blue pigment”, has long been considered a powerful adsorbent for radioactive cesium-137 from aqueous solutions due to its unique adsorption selectivity and high capacity. However owing to its

intrinsic property of forming a colloid in water that are notoriously difficult to handle in the process of liquid radioactive waste treatment; thus, practical applications have long been limited to medical and/or pharmaceutical treatments (G. B. Barton 1958).

Prussian blue was first synthesized by a Berlin color maker named Diesbach in 1704, at first this compound was only used as blue pigment for paints, lacquers or dyes due to the great intensity and stability of its color (Lopez-Palacios, Heras, Colina, and Ruiz, 2004). Nowadays, its applications range covers very different research areas such as sensors, biosensors (Arkady A. Karyakin 1995) (D. Moscone 2001), and electrocatalysis (F. Campus, 1999). In addition, the magnetic properties still aroused the applications of Prussian blue.

Prussian blue is usually synthesized by mixing Fe^{3+} with Fe (II) $(CN)6^{4-}$ or Fe^{2+} with Fe(III) $(CN)_6^{3-}$ giving a dark blue colloid. The basic structure of Prussian blue and Prussian blue analogues was first studied by Keggin and Miles (J.F. Keggin, 1936). Two types of Prussian blue had been reported. The "insoluble Prussian blue " $Fe(III)[Fe(III)Fe(II)(CN)6]_3$, and the "soluble Prussian blue", $A[Fe(III)Fe(II)(CN)_6]$, where A on behalf of alkali metal

(Shokouhimehr, Soehnlen, Khitrin, Basu, and Huang, 2010). A three-dimensional polymeric network consisted of the Prussian blue, where ferric and ferrous ions were alternated on cubic lattice sites linked by cyanide ligands. The Prussian blue structure is a cubic lattice with the Fe (II) and Fe (III) atoms occupying of the cube and the cyanide groups are placed at the sides. The Fe (II) atoms are bonded to the carbon atom in the cyanide group and the Fe (III) atoms are bonded to the nitrogen atom in the cyanide group. The residual charge was balanced either by ferric ions or by alkali actions (López-Palacios, Heras, Colina, and Ruiz, 2004). Additionally there are typically 14-16 water molecular coordinated to the Prussian blue molecule (Ricci, and Palleschi, 2005). The color of Prussian blue is due to the electronic transition from a low spin Fe (II) ion in a carbon coordination center, to a high spin Fe (III) ion in a nitrogen coordination Centre, that occurs when visible light is absorbed at around 700 nm (Lopez-Palacios *et al.*, 2004). The zeolitic nature of Prussian blue with a cubic unit cell of 10.2 $\overset{0}{A}$ allows the diffusion of low molecular weight molecules (such as Cs^{+}) through the crystal (Ricci *et al.*, 2005).

However, due to its intrinsic property of forming a colloid in water, small sized Prussian blue particles thereby the larger surface areas and the higher adsorbing capacity can easily contaminate water; thus, practical applications have long been limited to medical and/or pharmaceutical treatments (P.J. Faustino, 2008) (B.L. Gall, 2006). Note that some Prussian blue analogs, like cobalt ferrocyanide (W.E. Prout, 1965) (Raouf, 2003) and copper ferrocyanide (E.F.T. Lee, 1983), are highly water-insoluble; can be used directly as adsorbents for radioactive cesium eliminations. However, these analogs are costly compared to Prussian blue. Moreover, the procedures for isolating particles of desirable sizes are typically time-consuming, because impurities and smaller particles must be removed from the suitable particles. This is typically achieved by washing the mixtures with large amounts of water, followed by centrifugation. Considerable effort has been devoted to the development and optimization of procedures using Prussian blue.

Usually PB is obtained as fines, which have superior sorption properties due to high surface area and fast kinetics, but are notoriously difficult to handle because of the character of forming the colloidal problem in the process of liquid radioactive waste treatment. To overcome this disadvantage,

column applications are the common methods, however, often at the expense of sorption capacity loss and much slower kinetic of cesium removal. Thus a new method should be developed to overcome the colloidal problem.

1.4 Aim of this study

The elimination of low-level radioactive cesium from a certain contaminated environment is one of the most important tasks towards achieving the goal of environmental remediation. A high-capacity, low-cost adsorbent whose volume can be easily reduced after adsorption is required. In order to satisfy these requirements, Prussian blue (Ferric hexacyanoferrate) has long been considered as a powerful absorbing element for elimination of radioactive cesium due to its unique adsorption selectivity and the high capacity. However, due to its intrinsic property of forming a colloid in water, small sized Prussian blue particles can easily contaminate water; thus, practical applications have long been limited to the medical and/or pharmaceutical treatments.

For several years, we have been developing caged approaches to overcome the difficulty associated with colloidal dispersion. We have tested organic polymers (like alginate) and porous inorganic particles (like diatomite) as

potential caging materials to create high-performance adsorbent(Yu, and Fugetsu, 2010). In this study, we demonstrated that the caging approach can be applied to Prussian blue to create an absorptive structure with high efficiency, as well as a low-cost, character of self-uptake of water and after the volume can be easily reduced after the adsorption; named polymers NB-9000B used as the binder, to create high-performance spongiform adsorbents for eliminating the radioactive cesium from low level radioactive water.

1.5 References

Newspaper article (Yomiuri online): Govt, TEPCO announce new road map on N-crisis; http//www.yomiuri.co.jp/dy/national/T110720005363.httm

(1980). Management of persons accidentally contaminated with radionuclides. *National Council on Radiation Protection and Measurements. NCPR report* 65, 77.

Arkady A. Karyakin , Olga V. Gitelmacher, Elena E. Karyakina. (1995). Prussian Blue-Based First-Generation Biosensor. A Sensitive Amperometric Electrode for Glucose. 67 2419–2423.

B.L. Gall, F. T., D. Renault, J. C. Wilk, E. Ansoborlo, . (2006). Comparison of Prussian blue and apple-pectin efficacy on 137Cs de-corporation in rats. *Biochimie* 88 1837-1841.

Bystrzejewska-Piotrowska, G., and Bazała, M. A. (2008). A study of mechanisms responsible for incorporation of cesium and radiocesium into fruitbodies of king oyster mushroom (Pleurotus eryngii). *Journal of Environmental Radioactivity* 99, 1185-1191.

C.E. Miller, L. D. M. (1956).

Science 124, 122–123.

Cortes-Martinez, R., Olguin, M. T., and Solache-Rios, M. (2010). Cesium sorption by clinoptilolite-rich tuffs in batch and fixed-bed systems. *Desalination* 258, 164-170.

D. Moscone , D. D. O., D. Compagnone , and G. Palleschi. (2001). Construction and Analytical Characterization of Prussian Blue-Based Carbon Paste Electrodes and Their Assembly as Oxidase Enzyme Sensors. *Anal. Chem.* 73, 2529–2535.

Ding, D., Zhao, Y., Yang, S., Shi, W., Zhang, Z., Lei, Z., and Yang, Y. (2013). Adsorption of cesium from aqueous solution using agricultural residue – Walnut shell: Equilibrium, kinetic and thermodynamic modeling studies. *Water Research* 47, 2563-2571.

E.F.T. Lee, M. S. (1983). Sorption of cesium by complex hexacyanoferrates III. A study of the sorption properties of potassium copper ferrocyanide, . *J. Chem. Tech. Biotechnol* 33, 80-86.

F. Campus, P. B. t., M. Gra tze, S. Heinen, L. Walder. (1999). Electrochromic devices based on surface-modi Ped nanocrystalline TiO_2 thin- Plm electrodes. *Solar Energy Materials & Solar Cells* 56 281-297.

G. B. Barton , J. L. H., E. D. McClanahan , R. L. Moore , H. H. Van Tuyl.

(1958). Chemical Processing Wastes. Recovering Fission Products. *Industrial & Engineering Chemistry* 50 212–216.

G.Brumfiel. (2011). Fukushima set for epic clean-up. *nature* 472, 146-147.

J.F. Keggin, D. D. M. (1936). Structure and formula of the prusian blue and related compounds. *Nature* 577,

López-Palacios, J., Heras, A., Colina, Á., and Ruiz, V. (2004). Bidimensional spectroelectrochemical study on electrogeneration of soluble Prussian Blue from hexacyanoferrate(II) solutions. *Electrochimica Acta* 49, 1027-1033.

Laboratory, A. N. (2005). cesium. *Human health fact sheet*

Lopez-Palacios, J., Heras, A., Colina, A., and Ruiz, V. (2004). Bidimensional spectroelectrochemical study on electrogeneration of soluble Prussian Blue from hexacyanoferrate(II) solutions. *Electrochimica Acta* 49, 1027-1033.

Manolopoulou, M., Stoulos, S., Ioannidou, A., Vagena, E., and Papastefanou, C. (2013). Radioecological indexes of fallout measurements from the Fukushima nuclear accident. *Ecological Indicators* 25, 197-199.

P.J. Faustino, Y. Y., J.J. Progar, C.R. Brownell, N. Sadrieh, J.C. May, E. Leutzinger, D.A. Place, E.P. Duffy, F. Houn, S.A. Loewke, V.J. Mecozzi, C.D. Ellison, M.A. Khan, A.S. Hussain, R.C. Lyon,,. (2008). Quantititave

determination of cesium binding to ferric hexacyanoferrate: Prussian blue. *J. Pharm. And Biomed. Anal* 114-125.

Pinsky, C., and Bose, R. (1984). Pharmacological and Toxicological Investigations of Cesium. *Pharmacology Biochemistry and Behavior* 21, 17-23.

Raouf, M. A. (2003). Potassium hexacyanocobalt ferrate and ammonium molybdophosphate sorption bags for the removal of 137Cs from aquepus solutions and simulated waste. *J. Chem. Tech. Biotechnol* 79, 22-29.

Ricci, F., and Palleschi, G. (2005). Sensor and biosensor preparation, optimisation and applications of Prussian Blue modified electrodes. *Biosensors & Bioelectronics* 21, 389-407.

Rogers, H., Bowers, J., and Gates-Anderson, D. (2012). An isotope dilution-precipitation process for removing radioactive cesium from wastewater. *Journal of Hazardous Materials* 243, 124-129.

Sangvanich, T., Sukwarotwat, V., Wiacek, R. J., Grudzien, R. M., Fryxell, G. E., Addleman, R. S., Timchalk, C., and Yantasee, W. (2010). Selective capture of cesium and thallium from natural waters and simulated wastes with copper ferrocyanide functionalized mesoporous silica. *Journal of Hazardous*

Materials 182, 225-231.

Sawidis, T., Heinrich, G., and Brown, M.-T. (2003). Cesium-137 concentrations in marine macroalgae from different biotopes in the Aegean Sea (Greece). *Ecotoxicology and Environmental Safety* 54, 249-254.

Shokouhimehr, M., Soehnlen, E. S., Khitrin, A., Basu, S., and Huang, S. D. (2010). Biocompatible Prussian blue nanoparticles: Preparation, stability, cytotoxicity, and potential use as an MRI contrast agent. *Inorganic Chemistry Communications* 13, 58-61.

Steefel, C. I., Carroll, S., Zhao, P., and Roberts, S. (2003). Cesium migration in Hanford sediment: a multisite cation exchange model based on laboratory transport experiments. *Journal of Contaminant Hydrology* 67, 219-246.

Sukwarotwat, T. s. V. (2010). Selective Capture of Cesium and Thallium from Natural Waters and Simulated Wastes with Copper Ferrocyanide Functionalized Mesoporous Silica. *Hazardous Materials* 182, 225-231.

Volchek, K., Miah, M. Y., Kuang, W. X., DeMaleki, Z., and Tezel, F. H. (2011). Adsorption of cesium on cement mortar from aqueous solutions. *Journal of Hazardous Materials* 194, 331-337.

W.E. Prout, E. R. R., H.J. Groh,J (1965). Ion exchange absorption of cesium

by potassium hexacyanocobalt (II) ferrate (II), . *Inorg. Nucl. Chem* 27 473-479.

Yoshida, S., Muramatsu, Y., Dvornik, A. M., Zhuchenko, T. A., and Linkov, I. (2004). Equilibrium of radiocesium with stable cesium within the biological cycle of contaminated forest ecosystems. *Journal of Environmental Radioactivity* 75, 301-313.

Yu, H. W., and Fugetsu, B. (2010). A novel adsorbent obtained by inserting carbon nanotubes into cavities of diatomite and applications for organic dye elimination from contaminated water. *Journal of Hazardous Materials* 177, 138-145.

Zhang, C. P., Gu, P., Zhao, J., Zhang, D., and Deng, Y. (2009). Research on the treatment of liquid waste containing cesium by an adsorption-microfiltration process with potassium zinc hexacyanoferrate. *Journal of Hazardous Materials* 167, 1057-1062.

Chapter II

The caging of Prussian blue into the cavities of diatomite adopt an in situ micro-packing approach

2.1 Introduction

2.1.1 Diatomite

Diatomaceous earth (DE) or diatomite is a siliceous, sedimentary rock resulting from the siliceous fossilized skeleton and available in large deposits around the world that existed during tertiary and quaternary periods (van Garderen, Clemens, Mezzomo, Bergmann, and Graule, 2011). It was composed of rigid cell walls, called frustules. The dimensions of frustule were from less than 1 um to more than 100 um, according to the different species. The organism through filtration of silica from water formed these cell walls and referred to as the skeleton of the organism. The principally of this organism was consisted of silicon dioxide (SiO_2) often greater than 85%, with small amount of alumina (Al_2O_3) and ferric oxide (Fe_2O_3) (Tsai, Lai, and Hsien, 2006). As a result, diatomite is both odourless and non-toxic and the naturally occurred abundance with high purities. Consequently, the diatomite is available at low cost.

In fact, diatomite is highly porous, with its structure containing up to 80–90% voids (Khraisheh, Al-degs, and McMinn, 2004). Particular interested in diatomite was due to its unique properties such as: small

particle size (diameter was belonging to micro meter), high porosity, high permeability, low thermal conductivity, and chemical inertness. Due to the highly porous structure of diatomite, some authors have mentioned that diatomite is regarded as a cheap material with attractive mechanical resistance that can be used as a filter, filler or mild abrasive material (van Garderen *et al.*, 2011). The early utilization of diatomite for water purification was based on these specific properties. In the Second World War, the ground troops of US were equipped with a portable diatomite filter system to produce the suitable drinking water from the contaminated water (de Namor, El Gamouz, Frangie, Martinez, Valiente, and Webb, 2012).

Currently, diatomite has extensively been applied in a number of industrial applications, e.g. as a filtration media for inorganic and organic chemicals (Al-Ghouti, and Al-Degs, 2011), as an adsorbent for the extraction of arsenic, mercury and the other heavy metals from water (van Garderen *et al.*, 2011) (Al-Ghouti, Khraisheh, and Tutuji, 2004; de Namor *et al.*, 2012). Owing to some unique combination of physical and chemical properties, application of diatomite as an adsorbent in wastewater treatment has not been extensively investigated.

In this study, the diatomite was used as a micro-meter sized container for storage of the in situ synthesized Prussian blue particles. Prussian blue (Ferric hexacyanoferrate) has long been considered as a powerful absorbing element for elimination of radioactive cesium due to its high binding capacity to cesium in the aqueous solution. However, its intrinsic property of forming a colloid in water, and different to handle in the process of post treatment, thus, practical applications have long been limited. In this study, we have developed a caging approach to overcome the intrinsic difficulties associated with colloidal dispersion of Prussian blue in water to create high-performance spongiform adsorbents for eliminating the radioactive cesium from low level radioactive water.

For several years, we have been developing caged approaches to overcome the difficulties associated with colloidal dispersion. We have tested organic polymers (like alginate) and porous inorganic particles (like diatomite) as potential caging materials to create high-performance adsorbents (Fugetsu, Satoh, Shiba, Mizutani, Lin, Terui, Nodasaka, Sasa, Shimizu, Sato, Tohji, Tanaka, Nishi, and Watari, 2004; Yu, and Fugetsu, 2010). In this study, we demonstrated that the caging approach can be applied to Prussian blue to

create an absorptive structure with high efficiency for eliminating cesium-137 from low level radioactive water.

2.1.2 Discovery, property and applications of Carbon nanotubes

Carbon nanotubes (CNTs) have attracted enormous research attention in various scientific communities; since the first discovery in 1991 by Sumio Iijima as a by-product in the synthesis of fullerenes (Iijima, 1991). CNTs are a class of fullerenes structural family, consisting of a sheet of graphene rolled into small perfect cylindrical structures. Single-walled carbon nanotubes (SWCNTs) and multi-walled carbon nanotubes (MWCNTs) are the two main types of CNTs (Figure.2-1). SWCNTs can be supposed as long wrapped graphene sheets. MWCNTs have diameters significantly greater than SWCNTs.

CNTs are cylindrically sharped, sp^2 hybrid C=C bonds, entirely carbon materials. This sp^2 bonding structure is stronger than the sp^3 bonds and causes the molecules to have the unique strength. Nanotubes generally align themselves into aggregate state and held together by Van der Waals forces (Gharbavi, and Badehian, 2014). Their large surface area and shaper curvatures together with their high thermal and chemical stabilities make

them ideal for application to the adsorbent of pollutant chemicals, especially chemicals with aromatic backbones. By π-π stacking interactions between the aromatic backbones and hexagonal skeleton of CNTs was the predominant mechanism of the adsorption (Yu *et al.*, 2010).

CNTs have been at the frontier of nanotechnology research for the past two decades. They were considered one of the most promising reinforcement's materials. Individual CNTs possess exceptional combination of extreme mechanical and electrical properties. Therefore they are often considered as one of the best candidates for the reinforcement of the next generation of multifunctional composite materials (Wang, Bradford, Li, and Zhu, 2014) (Wei, Li, Xiong, Tan, Fan, Qin, and Zhang). Experiments indicated that the electrical and mechanical properties of the fibers could be improved by spinning CNTs incorporated with the fiber. According to the previous studies, when 3wt% CNTs was incorporated within the fibers, the strength and stiffness of the fibers were improved by 28% and 32%, respectively (Alvarez, Shanov, Ochmann, and Ruff, 2014; Baji, Mai, Abtahi, Wong, Liu, and Li, 2013).

In addition, CNTs can also be applied in the biological, such as drug

carriers for cancer treatment and as vaccine delivery vehicles, or as biosensors (A.M. Smith, 2009) (N.F. Reuel, 2012). However challenges still remain in the precise control CNTs into dispersed state from the aggregated state.

As a matter of fact, without compromising performance, the transfer of these extraordinary qualities into CNTs products, remains a challenge. The large scale application of CNTs was limited by dispersion technology and the possibility of leakage into the environmental. It is general known that CNTs were expensive previously; however, recent developments have demonstrated that CNTs can be mass produced at low price using catalytic chemical vapor deposition in fluidized bed reactor. This low-cost method paved a way to large scale manufacturing of CNTs (AE Agboola, 2007) (2012). Publications regarding the toxicities of CNTs toward plants, animal cells and/or tissues have been increasing rapidly, due to the fibrous shapes, CNTs have been compared to asbestos, raising great concerns that the widespread industrialization of such kind of the engineered nano-materials, and/or their subsequent products may lead to negative impacts to environmental surroundings and the biological systems. Early studies have shown that MWCNTs could induce granuloma, fibrosis, inflammation or decrease of

reactive oxygen species (ROS) in the animals and plants, warning further research and careful attentions on their potential toxicities (Bhattacharya, Andón, El-Sayed, and Fadeel, 2013) (Donaldson, Poland, Murphy, MacFarlane, Chernova, and Schinwald, 2013) (Kayat, Gajbhiye, Tekade, and Jain, 2011).

In this study, the dispersed CNTs were prepared by dispersing aggregated MWCNTs with a beads-milling system (Dyno-Mill, Basel, Switzerland) under zwitterionic surfactants as the wetting agent and sulfonated types of surfactants as the dispersants. The highly-dispersed CNTs were created over the surface of the diatomite as the purpose of sealing the Prussian blue particles; enhance the surface area and reinforcement the materials. A polyurethane polymer was employed as a binder to fasten the dispersed CNTs which created on the surface of the diatomite. Through this binding approach, the CNTs had been firmly entrapped into the polyurethane foam, and the possibility of leakage problem was in controlling. The resulting dried soft powders of CNTs-network/Diatomite/Prussian blue composites were immobilized on the cell walls of the polyurethane form for adsorbing cesium ions in the wastewater treatment.

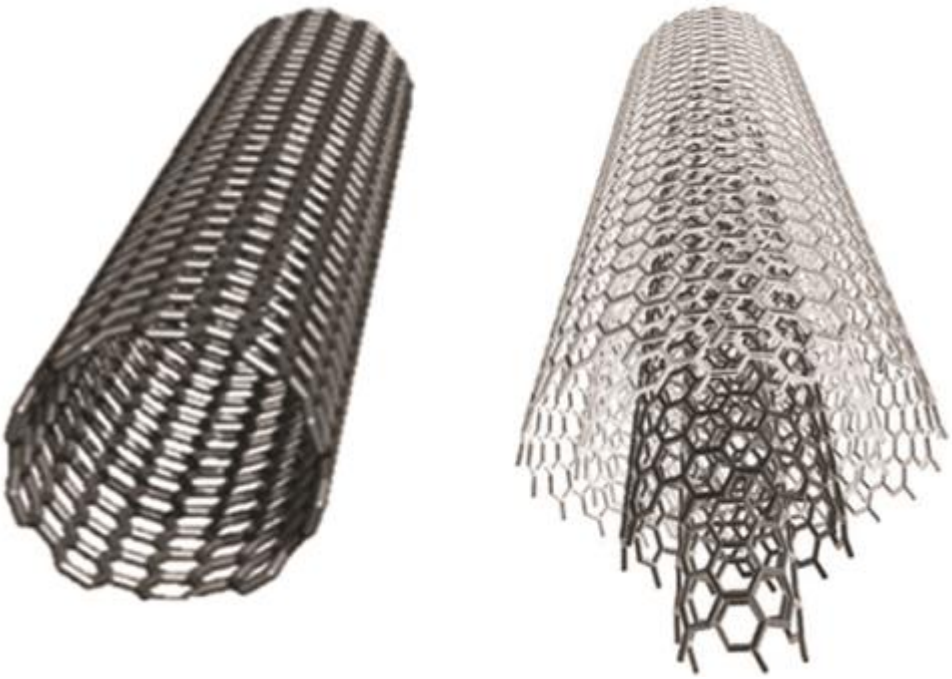

Figure 2-1. Single (left)-and multi-walled (right) carbon nanotubes

2.2 Experiment

2.2.1 Materials and reagents

Powders of diatomite, MW-27, obtained from Eagle-Picher Filtration & Minerals, Inc., U.S.A.; average particle diameter, 13um; bulk specific gravity, 0.19 g/cm^3; as recommended by the manufacture.

Multi-walled carbon nanotubes; trade name, Nanocyl-7000, Belgium; average diameter 9.5 nm, average length 1.5um and, Brunauer–Emmett–Teller specific surface area 250-300 m^2/g, as suggested by the manufacture.

$FeCl_3 \cdot 6H_2O$ and $Na_4Fe(CN)_6 \cdot 10H_2O$ were purchased from Wako. Other chemicals unless specifically noted were still from Wako Pure Chemical Industries, Ltd., or Sigma-Aldrich Inc., Japan.

2.2.2 Prussian blue synthesized in the cavities of diatomite

Prussian blue was synthesized within the cavities of diatomite with an in situ synthesizing process (Figure 2-2.). The diatomite was first washed thoroughly using deionized-water/methanol (50/50) to eliminate possible impurities, followed by filtration and drying at 100 °C. 750 g dried diatomite was mixed with an aqueous solution of 1000 mL 960 mM $FeCl_3 \cdot 6H_2O$ and 3000 mL de-ionized water with a mixer (FM-L, Nippon Coke & Engineering

Co., Ltd) for 2 hours. The resultant mixture (slurry) was heated at 90 °C in an oven to evaporate the water; the resulting fine powder (diatomite/$FeCl_3$ composite) was then slowly (approximately 30 minutes) added to an aqueous solution of 1000 mL 720 mM $Na_4Fe(CN)_6$ mixed with 3000 mL de-ionized water; the resulting slurry was then dried to fine powders at 90 °C. The standard Prussian blue fine powders were prepared with aqueous 960 mM $FeCl_3 \cdot 6H_2O$ and 720 mM $Na_4Fe(CN)_6$ solutions as the starting materials under the identical reaction conditions.

2.2.3 Prussian blue sealed in with carbon nanotubes

The diatomite/Prussian-blue fine powder was combined with 3000 mL of 2.0 wt% highly-dispersed CNTs and mixed gently for 10 min. The dispersed CNTs were prepared by dispersing multi-walled CNTs with a beads-milling system (Dyno-Mill, Basel, Switzerland) with zwitterionic surfactants as the wetting agent and sulfonated types of surfactants as the dispersants. The resulting slurry was then dried at 90°C to a fine powder.

2.2.4 Characterization

The samples were characterized by various techniques, such as Fourier transform infrared spectroscopy (FT-IR, FT/IR-6100 FTIR Spectrometer,

JASCO), scanning electron microscopy (SEM, JSM-6300, JOEL, with acceleration voltage of 30 kV), X-ray diffraction (XRD) using RINT2000, (Rigaku Denki Co. Ltd., Japan, X-ray $\lambda_{Cu\ K}\alpha$ =0.154 nm), and thermo gravimetric analysis (TGA, TG/DTA 6200, SII Exstar 6000, with heating rate of 5 K per minute under an air atmosphere).

2.3 Results and discussion

The diatomite used in this study had a cylindrical shape and ultra-high porosity; its maximum capacity for absorbing aqueous $FeCl_3 \cdot 6H_2O$ solution was 2.5 ml solution/g diatomite. This was found to be optimal, irrespective of the $FeCl_3$ concentration. Figure 2-3 shows SEM images of the pristine diatomite in the order of different magnifications used for capturing iron (III) chloride. Diatomite frustules are mainly divided into two categories; centric (discoid) and pennate (elongated to filiform). The Figure 2-3. Indicated both types of diatomite were incorporated. It can be inferred from the SEM that the diatomite used in this study has a large void volume, in addition to its highly porous structure. The high porosity of this material was one of the main reasons for choosing it as a micro-miter container for synthesizing of Prussian blue particles (Khraisheh *et al.*, 2004).

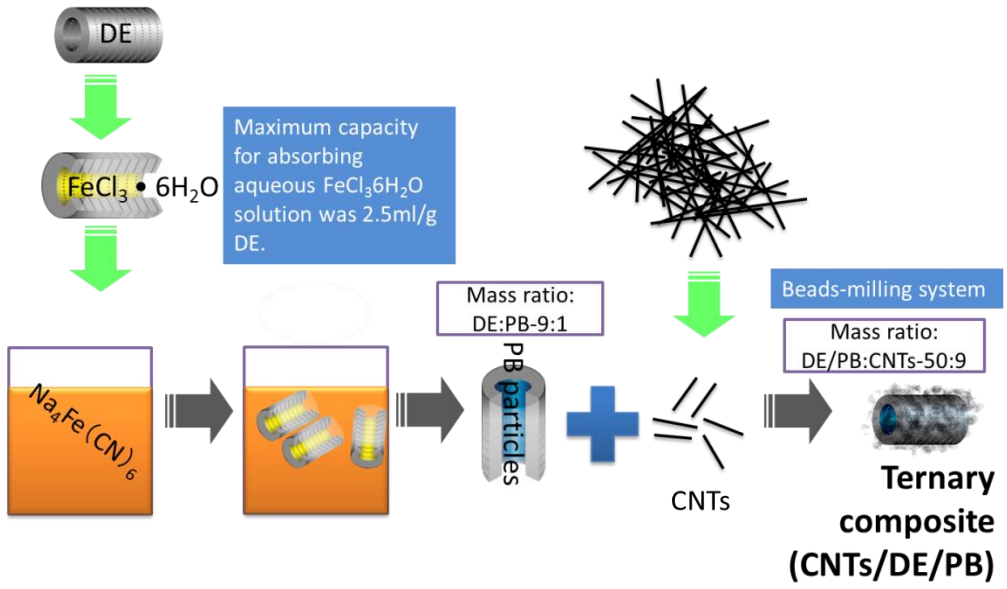

Figure 2-2. A schematic diagram of an in situ micro-packing approach

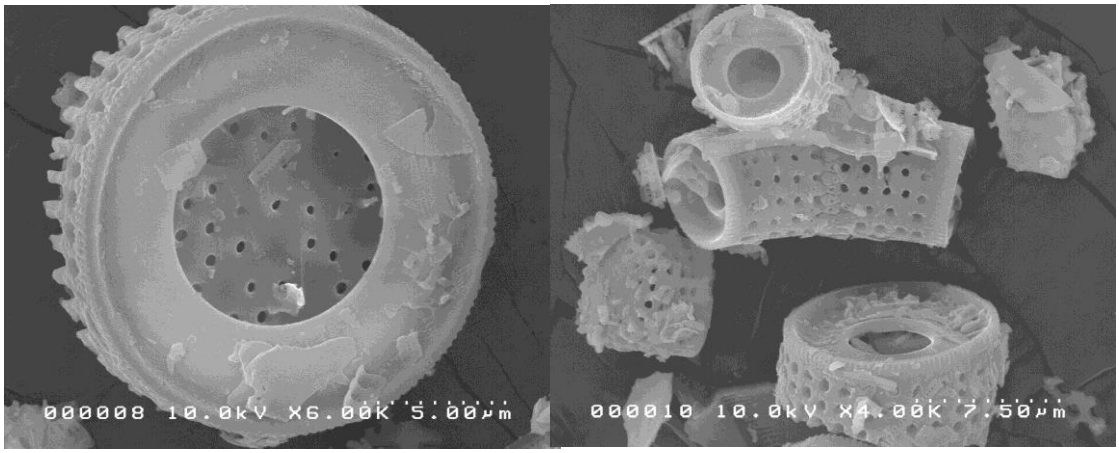

Figure 2-3. SEM images of the pristine diatomite used for capturing iron (III) chloride

Figure 2-4 shows typical SEM images of Prussian blue particles synthesized within the cavities of diatomite that through an in situ micro-synthesized approach. The Prussian blue particles were mostly found in diatomite cavities (very few Prussian blue particles were observed on the diatomite surface). Prussian blue particles had diameters of 10–150 nm, measured with transmission electron microscopy. Prussian blue particles packed in diatomite cavities were analyzed with X‑ray diffraction (XRD). Figure 2-5. Shows a typical XRD diffractogram; four main peaks were observed at scattering angles (2θ) of 17.44, 24.78, 35.34, and 39.54 which can be allocated to the Prussian blue phase (200, 220, 222 and 400) crystal planes respectively. These peaks were considered as relating to the face-centered cubic structure of Prussian blue with space group Fm3m. (Abdullahi Mohamed Farah, and and Ezekiel Dixon Dikio, 2012). Prussian blue is typically specified as either “soluble” or “insoluble”(B.M. Chadwick, 1966). This distinction is related to the presence or absence of an alkaline moiety (denoted as A’; in this study, A’ = Na) in the structural formula. Thus, $A'FeFe(CN)_6$ represents the soluble Prussian blue, and $Fe_4[Fe(CN)_6]_3$ represents the insoluble Prussian blue. The term “insoluble” is applicable only

to Prussian blues with a large particle size and a highly crystallized structure. These properties can be obtained by very slowly diffusing water vapor into a solution of Fe^{3+} and $Fe(CN)_6^{4-}$ in concentrated hydrochloric acid; however, this process is very time-consuming (generally, a few weeks are required) (H. J. BUSER, 1977). In this study, Prussian blues with structural formulas identical to a mixture Prussian blues, because they were produced in very short reaction times (30 min for 120 mmol Prussian blue); they were much smaller in diameter than the typical insoluble Prussian blues, and therefore, they had a tendency to readily disperse in water.

The UV-spectrum of the Prussian blue solution showed a broad absorption withλ_{max} at 700 nm. Figure 2-6 which is consistent with an intermetallic charge-transfer band from Fe^{2+} to Fe^{3+} in Prussian blue (Liu, 2009). This character can be used to confirm the whether Prussian blue particles dissolved in aqueous solution. Such as in this study, the achieved spongy form adsorption was washed with the deionized water, the squeezed deionized water was used to confirm the Prussian blue suspension. In order to investigate the functional groups of the synthesized Prussian blue particles, Fourier transform infrared spectroscopy (FT-IR) was employed to analysis the

sample. The sample for FT-IR measurement was in a KBr pellet at room temperature. The result was shown in Figure 2-7, the strong peak at 2084cm^{-1}, which is the characteristic absorption peak of Prussian blue and its analogues, can be attributed to stretching vibration of the cyanide group. The adsorption bands around 601 and 495cm^{-1} are due to the structure of Fe^{2+}-CN-Fe^{3+} linkage of Prussian blue structure. In additional, the adsorption bands near 3386 and 1610cm^{-1} refer to the O-H stretching mode and H-O-H bending mode, respectively, indicating the existence of the interstitial water in the sample (Loos-Neskovic, Ayrault, Badillo, Jimenez, Garnier, Fedoroff, Jones, and Merinov, 2004).

Prussian blue has several water molecules incorporated in its structure. The thermal decomposition of Prussian blue sample under air condition was conducted from the temperature range from 25 to 1000 ℃. Decomposition reaction is based on the release of cyanide group. The result was shown in Figure 2-8, four decomposition steps were observed including dehydration change of crystal structure of Prussian blue, and its decomposition. The thermogram showed four decomposition steps: I (25–240 ℃), II (240–350 ℃), III (350–550 ℃) and IV (550–1000 ℃) were agreed well with other thermal

studies of Prussian blue and Prussian blue analogs (Claudia Aparicio, 2011). In step I (25–240 ℃), the mass decreased was due to the water loss from the Prussian blue structure. In general, two types of water molecules are including, physically adsorbed water named zeolitic and chemically adsorbed named coordinating. The drying condition played the key role on number of zeolitic waters; while the number of coordinating waters is usually six. In this study, the sample of Prussian blue contained 16 water molecules at room temperature, which 10.5 were zeolitic and 5.5 were coordinating. This indicated the synthesized Prussian blue was a mixture between insoluble and soluble (Hitoshi MIMURA, 1997). Step II (240–350 ℃) described the decomposition of the cyanide group and formed the production of the intermediate. In step III (350–550 ℃) the mass decreased was probably due to the gas released from the intermediate such as NO_x, CO_2 and NH_3(Jukka Lehto, 1995) (J.I.Kunrath, 1987). Step IV (550–1000 ℃) pointed out that decomposition of the Prussian blue was almost completed at the temperature above 550 ℃ and yield the final product ferric oxide ($Fe_2O_{3)}$.

The dispersed CNTs were prepared by dispersing aggregated CNTs with beads-milling system with zwitterionic surfactants as the wetting agent and

sulfonated types of surfactants as the dispersants. The dispersed CNTs were directly confirmed by SEM and dynamic light-scattering size distribution, respectively. Figure 2-9 and Figure 2-10 are the typical data of the dispersed CNTs. The result of dynamic light-scattering size distribution of aqueous suspensions showed a typical particle size distributions' measurement for the dispersed CNTs suspension. 95% of the suspensions had been dispersed with the diameter below 100 nm, suggesting that the CNTs in the suspensions occurred at the tubular level for dispersion (Yu *et al.*, 2010).

The highly dispersed CNTs formed dense networks through their intrinsic self-assembly properties that coated the diatomite surfaces based on physical sorption (Figure 2-11). As a result, Prussian blue particles were prevented from diffusing out of the diatomite cavities. CNTs used in this study with the diameters possibly penetrate into the diatomite cavity. Few portions of the CNTs might undergo in this manner. The ratio of diatomite/Prussian-blue to CNTs (2.0 wt%) was optimized at 300 g/L.

The crystal phase structures of Prussian blue/diatomite composite and CNTs-network/diatomite/Prussian blue were characterized by X-ray diffraction patterns (XRD), the corresponding results are shown in Figure

2-12. The two XRD patterns are similar to each other, except for the peak at $2\theta =$ 26.3 º, which assigned to (0 0 2) planes of the CNTs (Zhu, Yao, Jiang, Fu, Wu, and Zeng, 2014) belong to the difference spectrum. The presence of (0 0 2) peak can be attributed to the sp^2 hybridization, carbon double bond (Favvas, Nitodas, Stefopoulos, Papageorgiou, Stefanopoulos, and Mitropoulos, 2014). The observed strong peak, in which $2\theta =$ 21.5 ºand 36 º are attributed to the diatomite, the other peaks are related to the PB particles that caged into the cavities of diatomite and sealed in with the dispersed CNTs.

Nitrogen adsorption isotherms of Prussian blue/diatomite composite and CNTs-network/diatomite/Prussian blue composite were shown in Figure 2-13. The CNTs provided the key role in the difference between the two samples. Both of the adsorption isotherms agreed well with the IUPAC type Ⅲ with hysteresis loop, which owing to the presence of the caged Prussian blue particles. The amount of the adsorption was increased above $P/P_0 = 0.9$ provided by creating dispersed CNTs on the surface of the diatomite, indicating a marked increase of the mesoporous porosity. According to the previous reference, by this mesoporous porosity, the cesium ions can

accelerate diffusion into the adsorbent sites, named caged Prussian blue. Moreover; CNTs-coated diatomite complex particles in the polyurethane spongiform, which the CNTs textures tightly banded the diatomite particles providing the porous should contribute to the anchoring (Tsuruoka, 2013). Moreover, the highly dispersed CNTs which created on the surface of the diatomite improved the corrosion resistant ability at the same time.

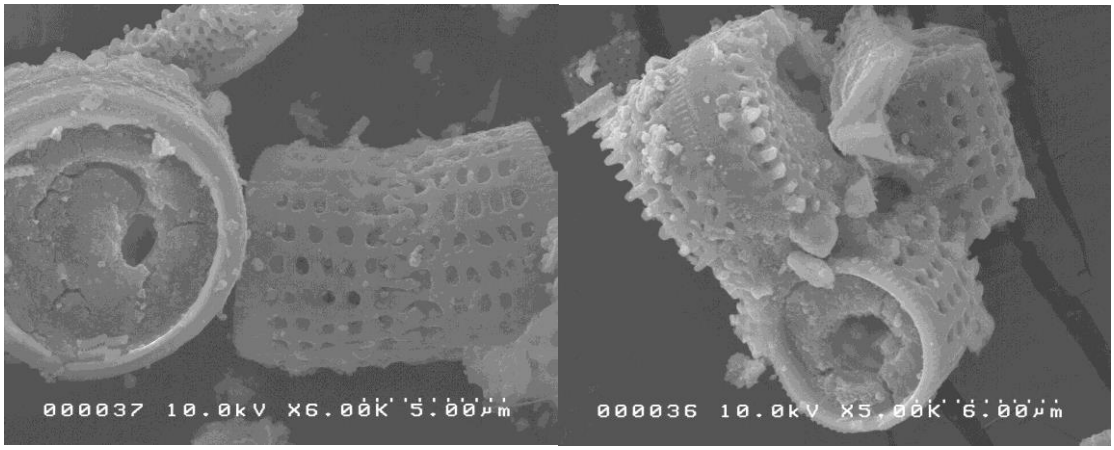

Figure 2-4. SEM images of the Prussian blue/diatomite composite.

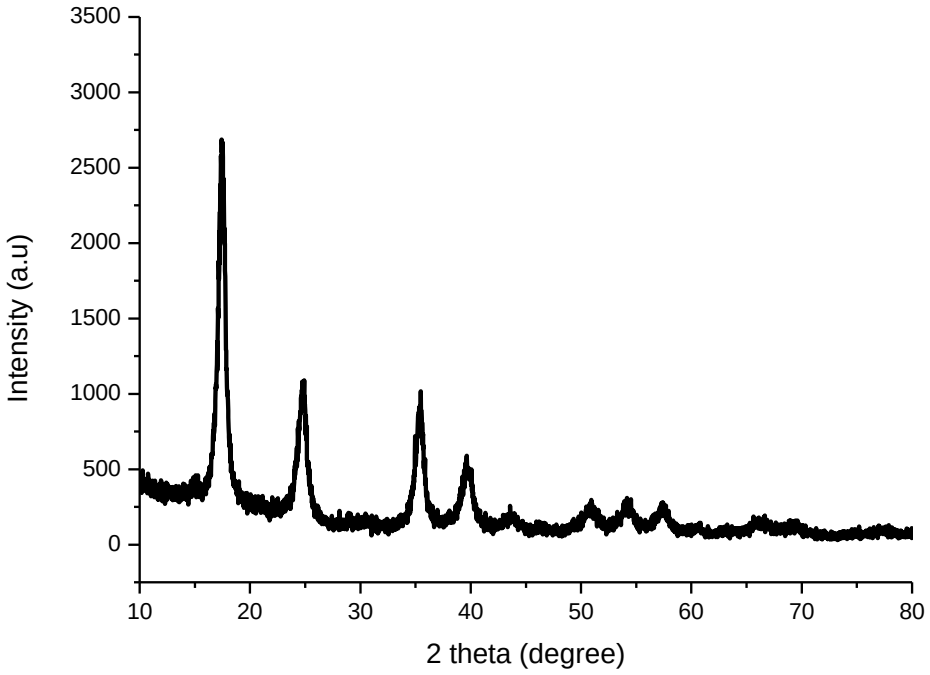

Figure 2-5. Typical XRD diffractogram of the Prussian blue particles.

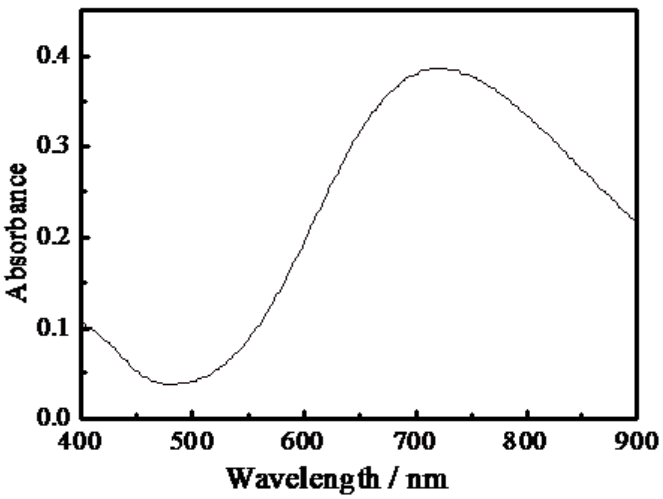

Figure 2-6. UV-vis spectra of Prussian blue dispersion.

(Prepared at molar ratio $Na_4Fe(CN)_6/FeCl_3$-3/4)

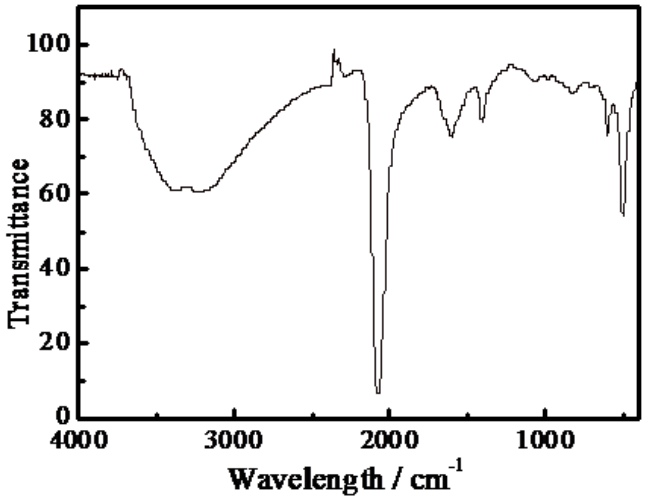

Figure 2-7. FT-IR spectra of Prussian blue particles.

(Prepared at molar ratio $Na_4Fe(CN)_6/FeCl_3$-3/4)

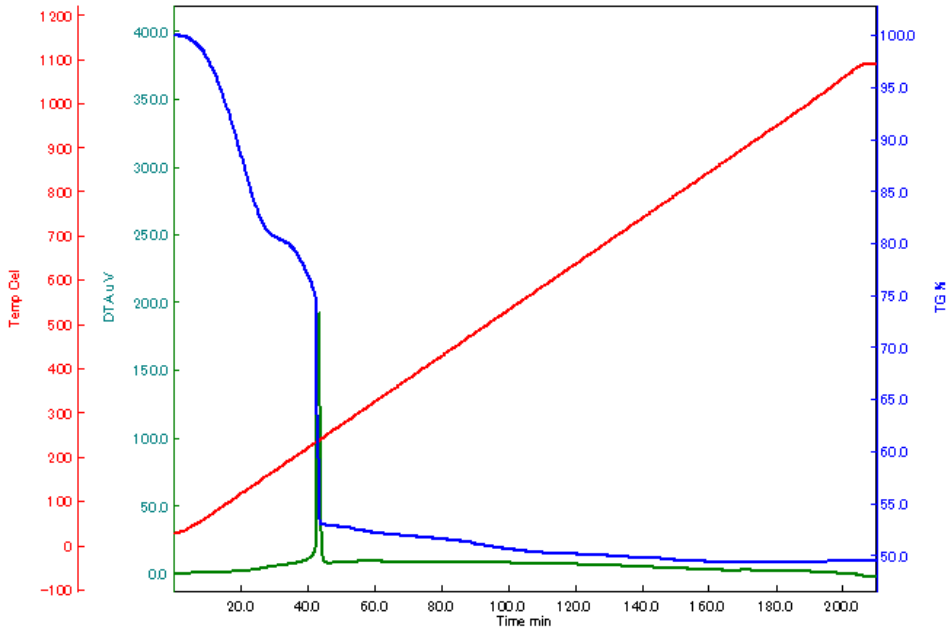

Figure 2-8. TG-A curve for the decomposition of Prussian blue particles.

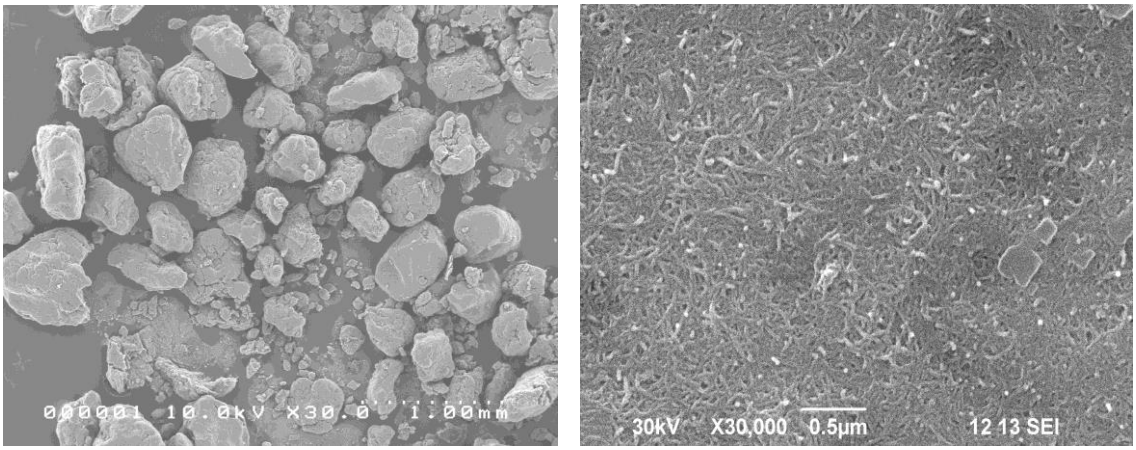

Figure 2-9. SEM images of the raw agglomerates of CNTs (left) and the agglomerate after being dispersed into the individual tubes (right).

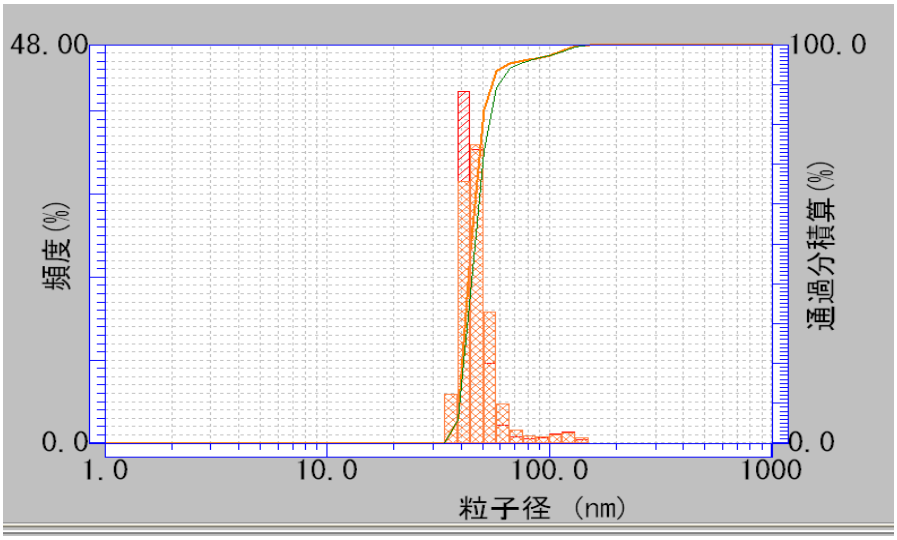

Figure 2-10. Dynamic light-scattering size distribution of the dispersed individual carbon nanotubes in the aqueous suspensions

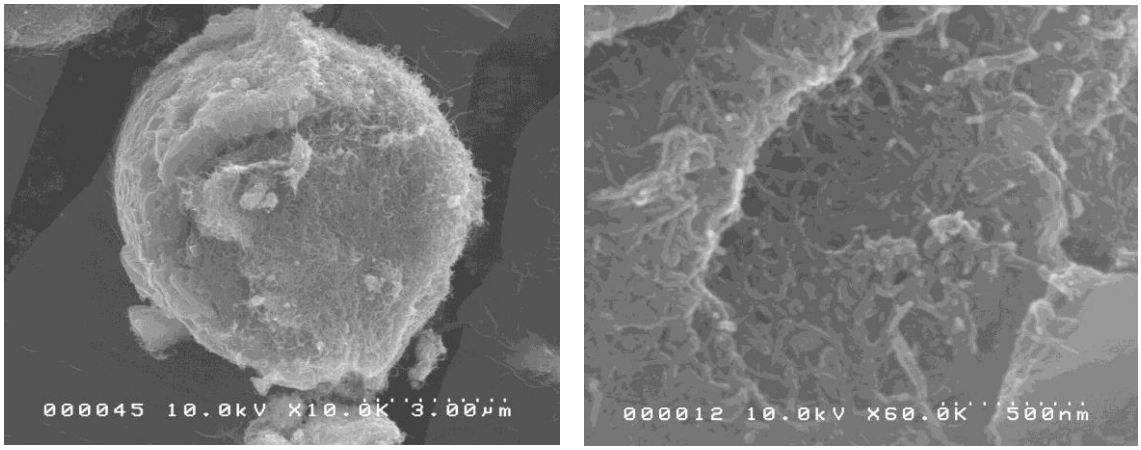

Figure 2-11. SEM images of the Prussian blue/diatomite surfaces were coated with highly dispersed CNTs. The CNTs formed a continuous interconnected network that prevented the diffusion of Prussian blue particles.

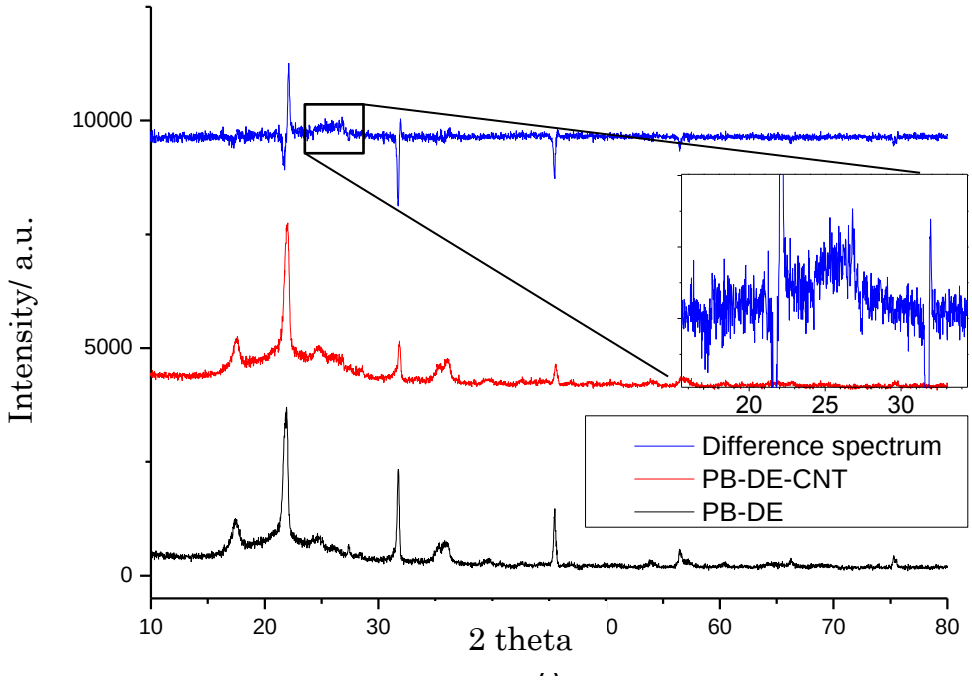

Figure 2-12. The powder X-ray diffraction patterns of Prussian blue/diatomite and CNTs-network/Prussian blue/diatomite samples

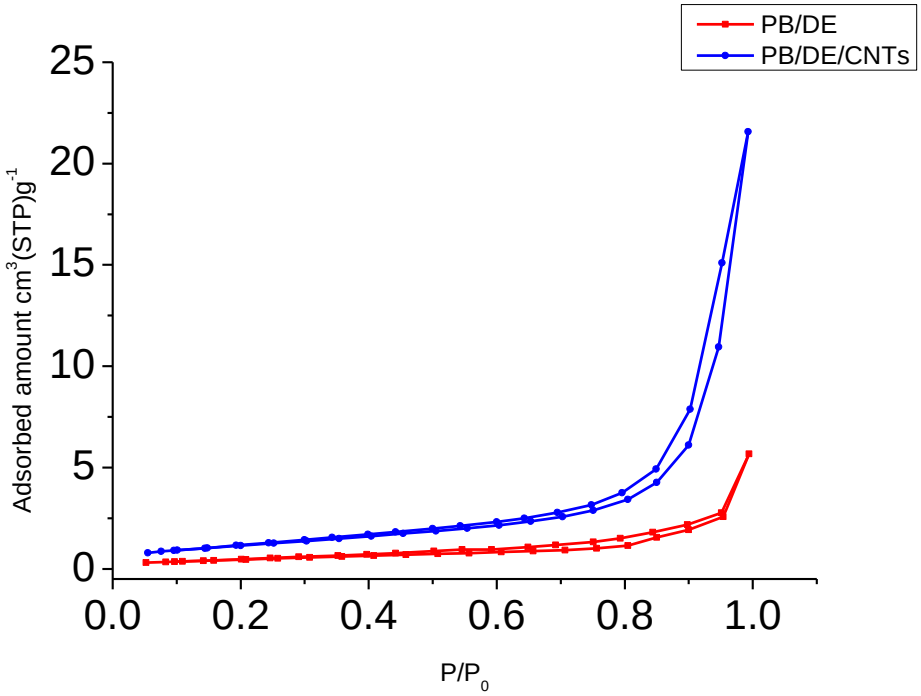

Figure 2-13. Nitrogen adsorption isotherms of Prussian blue/diatomite and CNTs-network/Prussian blue/diatomite samples.

2.4 Conclusion

We have demonstrated experimentally that adopt an easy to operate, highly efficient in situ micro-packing approach, Prussian blue particles could be produced with certain quantities in the cavities of diatomite, the results can be confirmed from SEM, BET, and XRD data. An additional nano sized network which consisted of highly dispersed CNTs was successful created over the surface of the diatomite; this CNTs-network has firmly sealed the Prussian blue particles inside the diatomite cavities and enhanced the surface area by increasing mesoporous porosity. CNTs; once being dispersed into individual tubes have shown high tendencies to form self-assembling interconnected networks; with the CNTs-network, the Prussian blue particles have been prevented from the possible diffusion from the diatomite cavities. Moreover, the CNTs-network have provided more contacting areas for the distribution of cesium and thereby enhancing water uptake into the absorbing element, namely, the caged Prussian blue.

2.5 References

(2012). Cheap Tubes Inc. http://www.cheaptubesinc.com/default.htm

A.M. Smith, M. C. M., S. Nie. (2009). Bioimaging: second window for in vivo imaging. *Nat Nanotechnol* 4, 710-711.

Abdullahi Mohamed Farah, N. D. S., Force Tefo Thema, Johannes Sekomeng Modise, and and Ezekiel Dixon Dikio. (2012). Fabrication of Prussian Blue/Multi-Walled Carbon Nanotubes Modified Glassy Carbon Electrode for Electrochemical Detection of Hydrogen Peroxide. *Int.J.Electrochem. Sci., Vol. 7, 2012* 7, 4302-4313.

AE Agboola, R. P., TA Hertwig, HH Lou. (2007). Conceptual design of carbon nanotube processes. *Clean Technologies and Environmental Policy* 9, 289-311.

Al-Ghouti, M. A., Khraisheh, M. A. M., and Tutuji, M. (2004). Flow injection potentiometric stripping analysis for study of adsorption of heavy metal ions onto modified diatomite. *Chemical Engineering Journal* 104, 83-91.

Al-Ghouti, M. A., and Al-Degs, Y. S. (2011). New adsorbents based on microemulsion modified diatomite and activated carbon for removing organic and inorganic pollutants from waste lubricants. *Chemical Engineering*

Journal 173, 115-128.

Alvarez, N. T., Shanov, V. N., Ochmann, T., and Ruff, B. (2014). Chapter 10 - Carbon Nanotube Fiber Doping. In *Nanotube Superfiber Materials* (Schulz, M. J., Shanov, V. N., and Yin, Z., eds.), pp. 289-311. William Andrew Publishing, Boston.

B.M. Chadwick, A. G. s. (1966). *adv. inorg.chem.Radiochem* 8, 83-89.

Baji, A., Mai, Y.-W., Abtahi, M., Wong, S.-C., Liu, Y., and Li, Q. (2013). Microstructure development in electrospun carbon nanotube reinforced polyvinylidene fluoride fibers and its influence on tensile strength and dielectric permittivity. *Composites Science and Technology* 88, 1-8.

Bhattacharya, K., Andón, F. T., El-Sayed, R., and Fadeel, B. (2013). Mechanisms of carbon nanotube-induced toxicity: Focus on pulmonary inflammation. *Advanced Drug Delivery Reviews* 65, 2087-2097.

Claudia Aparicio, L. M. a. Z. M. (2011). Thermal decomposition of Prussian blue under inert atmosphere. *Journal of Thermal Analysis and Calorimetry* 110, 661-669.

de Namor, A. F. D., El Gamouz, A., Frangie, S., Martinez, V., Valiente, L., and Webb, O. A. (2012). Turning the volume down on heavy metals using tuned

diatomite. A review of diatomite and modified diatomite for the extraction of heavy metals from water. *Journal of Hazardous Materials* 241, 14-31.

Donaldson, K., Poland, C. A., Murphy, F. A., MacFarlane, M., Chernova, T., and Schinwald, A. (2013). Pulmonary toxicity of carbon nanotubes and asbestos — Similarities and differences. *Advanced Drug Delivery Reviews* 65, 2078-2086.

Favvas, E. P., Nitodas, S. F., Stefopoulos, A. A., Papageorgiou, S. K., Stefanopoulos, K. L., and Mitropoulos, A. C. (2014). High purity multi-walled carbon nanotubes: Preparation, characterization and performance as filler materials in co-polyimide hollow fiber membranes. *Separation and Purification Technology* 122, 262-269.

Fugetsu, B., Satoh, S., Shiba, T., Mizutani, T., Lin, Y. B., Terui, N., Nodasaka, Y., Sasa, K., Shimizu, K., Akasaka, R., Shindoh, M., Shibata, K. I., Yokoyama, A., Mori, M., Tanaka, K., Sato, Y., Tohji, K., Tanaka, S., Nishi, N., and Watari, F. (2004). Caged multiwalled carbon nanotubes as the adsorbents for affinity-based elimination of ionic dyes. *Environmental Science & Technology* 38, 6890-6896.

Gharbavi, K., and Badehian, H. (2014). Structural and electronic properties of

armchair (7, 7) carbon nanotubes using DFT. *Computational Materials Science* 82, 159-164.

H. J. BUSER, l. D. (1977). The Crystal Structure of Prussian Blue: Fe4[Fe(CN)6]3*~H20 *Inorganic Chemistry Communications* 16, 2704-2710.

Hitoshi MIMURA, J. L. R. H. (1997). Chemical and Thermal Stability of Potassium Nickel Hexacyanoferrate (II). *Journal of Nuclear Science and Technology* 34, 582-587.

Iijima, S. (1991). Helical Microtubules of Graphitic Carbon. *Nature* 354, 56-58.

J.I.Kunrath, C. S. M. a. E. f. (1987). Thermal decomposition of potassium hexacyanoferrate (II) trihydrate. *Thermal analysis* 14, 253-264.

Jukka Lehto, M. p., juha Hinkula, . (1995). Gas evolved in the thermal decomposition of potassium cobalt hexacyanoferrate(II). *Thermochimica Acta* 265, 25-30.

Kayat, J., Gajbhiye, V., Tekade, R. K., and Jain, N. K. (2011). Pulmonary toxicity of carbon nanotubes: a systematic report. *Nanomedicine: Nanotechnology, Biology and Medicine* 7, 40-49.

Khraisheh, M. A. M., Al-degs, Y. S., and McMinn, W. A. M. (2004).

Remediation of wastewater containing heavy metals using raw and modified diatomite. *Chemical Engineering Journal* 99, 177-184.

Liu, Y. M. a. J. (2009). Assembly and electroanalytical performance of Prussian blue/polypyrrole composite nanoparticles synthesized by the reverse micelle method. *Science and Technology of Advanced MaterialsNational* 10, 10.1088/1468-6996/10/2/025001.

Loos-Neskovic, C., Ayrault, S., Badillo, V., Jimenez, B., Garnier, E., Fedoroff, M., Jones, D. J., and Merinov, B. (2004). Structure of copper-potassium hexacyanoferrate (II) and sorption mechanisms of cesium. *Journal of Solid State Chemistry* 177, 1817-1828.

N.F. Reuel, B. M., J. Zhang, A. Hinckley, M.S. Strano. (2012). Nanoengineered glycan sensors enabling native glycoprofiling for medicinal applications: towards profiling glycoproteins without labeling or liberation steps. *Chem Soc Rev* 41, 5744-5779.

Tsai, W.-T., Lai, C.-W., and Hsien, K.-J. (2006). Characterization and adsorption properties of diatomaceous earth modified by hydrofluoric acid etching. *Journal of Colloid and Interface Science* 297, 749-754.

Tsuruoka, S. F., Bunshi; Khoerunnisa, Fitri; Minami, Daiki; Takeuchi, Kenji;

Fujishige, Masatsugu; Hayashi, Takuya; Kim, Yoong Ahm; Park, Ki Chul; Asai, Michihiro; Kaneko, Katsumi; Endo, Morinobu. (2013). Intensive synergetic Cs adsorbent incorporated with polymer spongiform for scalable purification without post filtration. *Materials Express* 3, 21-29.

van Garderen, N., Clemens, F. J., Mezzomo, M., Bergmann, C. P., and Graule, T. (2011). Investigation of clay content and sintering temperature on attrition resistance of highly porous diatomite based material. *Applied Clay Science* 52, 115-121.

Wang, X., Bradford, P. D., Li, Q., and Zhu, Y. (2014). Chapter 23 - Aligned Carbon Nanotube Composite Prepregs. In *Nanotube Superfiber Materials* (Schulz, M. J., Shanov, V. N., and Yin, Z., eds.), pp. 649-670. William Andrew Publishing, Boston.

Wei, H., Li, Z., Xiong, D.-B., Tan, Z., Fan, G., Qin, Z., and Zhang, D. Towards strong and stiff carbon nanotube-reinforced high-strength aluminum alloy composites through a microlaminated architecture design. *Scripta Materialia*

Yu, H. W., and Fugetsu, B. (2010). A novel adsorbent obtained by inserting carbon nanotubes into cavities of diatomite and applications for organic dye

elimination from contaminated water. *Journal of Hazardous Materials* 177, 138-145.

Zhu, H. Y., Yao, J., Jiang, R., Fu, Y. Q., Wu, Y. H., and Zeng, G. M. (2014). Enhanced decolorization of azo dye solution by cadmium sulfide/multi-walled carbon nanotubes/polymer composite in combination with hydrogen peroxide under simulated solar light irradiation. *Ceramics International* 40, 3769-3777.

Chapter III

Fabrication of the spongiform adsorbents with the CNTs-network/ diatomite / Prussian blue as the functioning elements and the studies on the adsorptive behaviors

3.1 Introduction

3.1.1 Polyurethane

Polyurethane form (PUF) is an important class of polymer materials for a variety of applications due to their useful properties; such as excellent flexibility, elasticity and damping ability (Li, Li, Li, Yan, Wu, Cao, and He, 2013). PUF is copolymer-containing blocks of low molecular weight polyether covalently bonded by urethane group (-NHCOO-) (Moawed, and El-Shahat, 2013). The predominant reaction in PUF foam processing is polycondensation of poly-hydroxy compounds (polyols) with isocyanate. The two main classes of polyols are polyesterols and polyetherols. Eighty to ninety percent of polyols used today are polyetherols (Lefebvre, Bastin, Le Bras, Duquesne, Paleja, and Delobel, 2005).

The first paper reported the application of PUF was published in 1970 by Bowen. etc. for sorption of organic contaminants from water using a batch technique (Lemos, Santos, Santos, Santos, dos Santos, Souza, de Jesus, das Virgens, Carvalho, Oleszczuk, Vale, Welz, and Ferreira, 2007). This study resulted in a number of papers, involving the applications of PUF. In industry, the PUF foams are usually obtained by the reaction of an isocyanine and

polyol (or polyalcohol) in the presence of expansion agents, catalysts and surfactants (Neng, Pinto, Pires, Marcos, and Nogueira, 2007). PUF in particular is commonly chosen for the production of polymer foams because they can be tailored to meet the desired characteristics of the final products, varying the formulations used in their preparation. In the forms of foam, it is used in a wide range of industrial applications with worldwide production over a million tons per year (Rein, Lautenberger, Fernandez-Pello, Torero, and Urban, 2006). PUF has been widely used almost all commercial applications both in industry and in daily life.

The flexible PUF forms are widely used in a variety of commercially established applications because they are easy to handle and provide excellent cushioning and physical properties, especially in automotive seat cushions, as they can provide degrees of comfort and protection not achieved by any other single material (Deng, Davies, and Bajaj, 2003). PUF served as an excellent matrix for polymeric composite materials still (Xiong, Zheng, Qin, Li, Li, and Wang, 2006).

The importance of polyurethane foam has been increased as collector materials and excellent possibility to insert solids in the foam structure and

firmly retaining various loading and extracting agents. Furthermore, PUF present appropriate characteristics, in particular high thermal stability, simplicity and speed of synthesis, and low cost (Neng *et al.*, 2007), which is convenient for field studies (El-Shahat, Moawed, and Burham, 2008). Therefore, this high available cellular structure possible provided the PUF as an excellent material which is suitable for different extraction applications.

3.2 Experiment

3.2.1 Materials and reagents

Polyurethane prepolymer NB-9000B: A typical polyurethane prepolymer, derived from poly (oxy C2-4 alkylene) diol and toluene diisocyanate. It has three isocyanate functionalities, and it is capable of forming spongiform structures when combined with water molecules. In this study, NB-9000B was used as the binder for preparing the flexible, foam type of the adsorbent, was provided by INOAC Corporation.

Pluronic L-62, a tri-block type of copolymer, was used to strengthen the cell walls of the polyurethane foam (i.e., spongiform structure). The ratio of ternary-composite-powder/NB-9000B/Pluronic-L-62 was optimized at

10/100/1. Other chemicals unless specifically noted were from Wako Pure Chemical Industries, Ltd., or Sigma-Aldrich Inc., Japan.

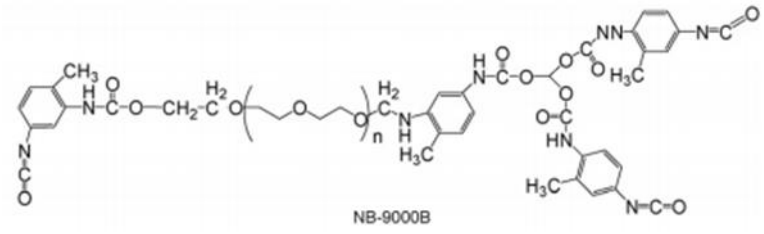

R-NCO + HO-R' → R-NHCOO-R' (a)

R-NCO + H_2O → [R-NHCOOH] → R-NH_2 + CO_2 (b)

RNCO + R-NHCOO-R' → R-N(CONHR)COO-R' (c)

Figure 3-1 Structures of the polyurethane prepolymer, NB-9000B, and the reactions involved in the polyurethane foam formation:

(a) chain extension reaction

(b) foam formation reaction and

(c)cross-linking reaction

3.2.2 Fabrication of the spongiform adsorbents with the CNTs-network/diatomite/Prussian blue as the functioning elements

The ternary composite fine powders (diatomite with Prussian blue in the cavities sealed in with highly-dispersed CNTs) was mixed with polyurethane prepolymer NB-9000B to produce the spongiform, Prussian blue based adsorbent.

3.2.3 Adsorption section

Chemical behavior of radioactive cesium-137 is expected to be almost identical to that of inactive cesium-133; analyses of stable Cesium-133 could be useful to understand the long-term behavior of radioactive and its equilibrium distribution.

Elemental, inactive cesium (cesium-133) was used to study adsorption behaviors. The quaternary spongiform matrix (polyurethane polymer, CNTs, diatomite, and Prussian blue), Prussian blue based adsorbent (in this study, denoted as PUF/CNTs/DE/PB) was cut into small pieces (approximately 0.1 g, dry weight) and then immersed in 40 mL aqueous cesium nitrate solution. The test tubes were then shaken on a vortex shaker. The amount of cesium that remained in solution was quantified with inductively-coupled plasma, atomic

emission spectrometry (ICP-AES; ICP-AES-9000, Shimadzu). In addition, radioactive cesium-137 was used as the targeted species at low concentrations. The adsorption of each sample was tested in triplicate, and averages were used to evaluate adsorbent capabilities.

3.2.4 Characterization

The samples were characterized by various techniques, such as scanning electron microscopy (SEM, JSM-6300, JOEL, with acceleration voltage of 30 kV), inductively coupled plasma, atomic emission spectrometry (ICP-AES-9000, Shimadzu), surface morphological analyzer (a keyence VK-X 100/X 200 system).

3.3 Results and discussions

3.3.1 Fabrication of the spongiform Prussian blue based adsorbents

The ternary (CNTs-network/diatomite/Prussian blue) composite was finally immobilized in the cell walls of the polyurethane matrix. Figure 3-2 shows typical SEM images of the PUF/CNTs/DM/PB spongiform, Prussian-blue based adsorbent system. This spongiform adsorbents were confirmed by washing the PUF/CNTs/DM/PB quaternary spongiform adsorbent system with de-ionized water, and then analyzing the washed water

for released Prussian blue with a UV-vis spectrometer. Prussian blue was not detected in the washed water; this phenomenon indicated that Prussian blue was firmly immobilized in the spongiform adsorbent.

3.3.2 Effects of CNTs and diatomite on cesium adsorption

Adsorption experiments were conducted in duplicate with aqueous solutions that contained 10.0 ppm cesium-133 as the targeted species. The adsorbents were the PUF/CNTs/DM/PB quaternary composite and the ternary (PUF/DM/PB) composite, with and without the CNT-based coating, respectively. Figure 3-3 shows the levels of cesium-133 detected in the solution after the adsorption. The PUF/CNTs/DM/PB adsorbent showed an elimination efficiency of 57.7%. Elimination efficiency was calculated as $(C-C_0)/C_0$, where C denotes the concentration of residual free cesium after adsorption, and C_0 denote the initial cesium concentration. The PUP/DM/PB adsorbent gave an elimination efficiency of 47.2%. Thus, the elimination efficiency of the PUF/CNTs/DM/PB adsorbent was 10.5% higher than that of the PUF/DM/PB adsorbent under identical experimental conditions. Moreover, the PUF/CNTs/DM/PB adsorption equilibrated within 2 h, and the PUF/DM/PB adsorption required 5 h for equilibration. The surface roughness

of the spongiform adsorbents was analyzed with a surface morphological analyzer (a Keyence VK-X 100/X 200 system). Figure 3-4 shows that the PUF/CNTs/DM/PB adsorbent had a rougher surface than the PUF/DM/PB adsorbent. Because the rougher surface of the PUF/CNTs/DM/PB adsorbent might have provided more contact areas for the distribution of cesium ions into the spongiform structure, this may have contributed to the higher elimination efficiency. Furthermore, a previous study showed that, when CNTs penetrated into a vegetable organism, they enhanced plant growth by enhancing water absorption(M. Khodakovskaya, 2009). In the present study, the PUF/CNTs/DM/PB absorbent was coated with a homogenous distribution of CNTs. Thus, like the plant system, this coating most likely enhanced water uptake into the spongiform matrix (M. Khodakovskaya, 2009). Note here that the entire CNTs in the powders form were tested as adsorbent for absorption of cesium from the water samples; a significant change (> 3%) in cesium concentration was not observed. In other words, the entire CNTs were found to have no or very little ability for the cesium adsorption.

For the diatomite, their filtration characteristics are particularly significant. In a previous study, a naturally occurred diatomite after being ground into 60

mesh fine powders were used for adsorption of three radionuclides (Cs-137, Cs-134 and Co-60) (Osmanlioglu, 2007). A pilot-scale, column-type device was established; it was found to be capable of reducing the radioactivity from the initial 2.60 Bq/ml to 0.40 Bq/ml within about 8 days, for a certain liquid waste sample. In our study, the diatomite was used to serve as micro-meter sized containers for the storage of the Prussian blue particles. Diatomite once being embedded in the spongiform materials showed very little ability (< 2%) for absorbing cesium.

A

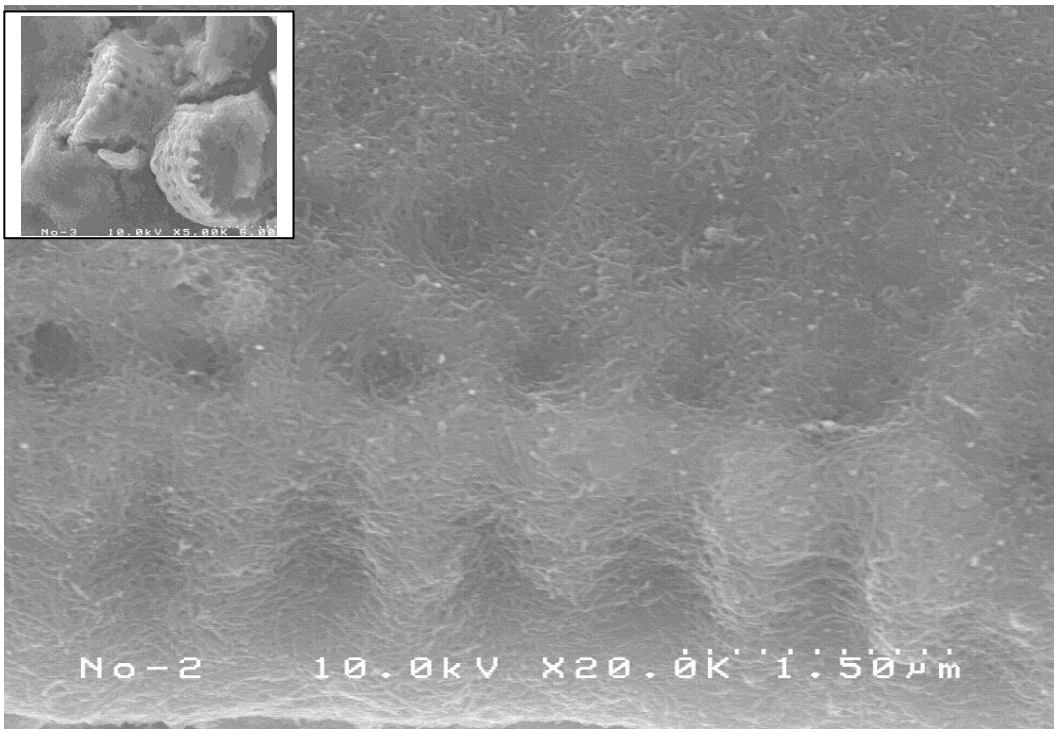

B

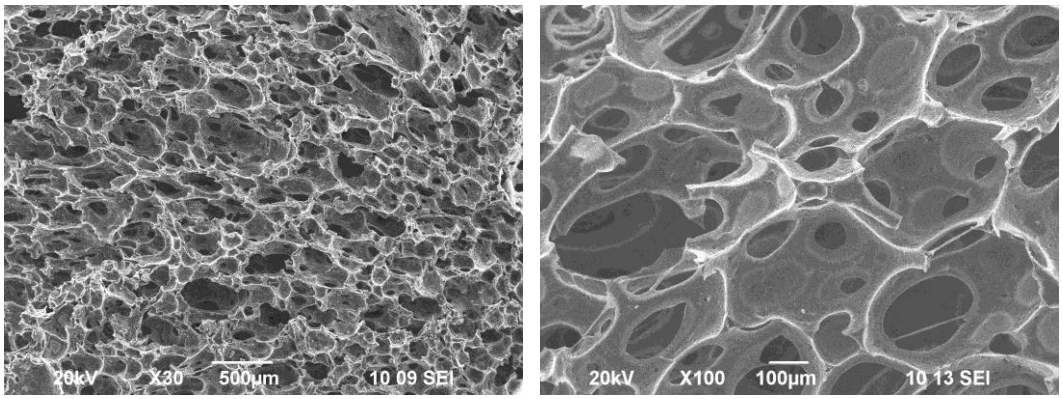

Figure 3-2. (A) Prussian blue was sealed into the cavities of the diatomite (upper, lower resolution). The diatomite surfaces were coated with highly dispersed multi-walled CNTs (upper, high resolution). (B) Representative SEM images of the quaternary (PUF/CNTs/DM/PB), spongiform, Prussian blue based adsorbent (left, ×30 magnification; right, ×100 magnification).

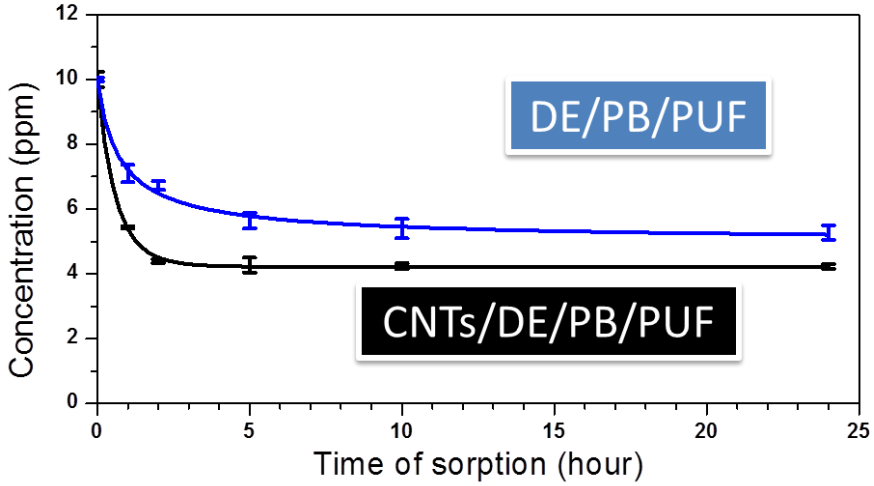

Figure 3-3. Concentrations of residual cesium-133 in the aqueous solution as a function of the time of adsorption. Blue line represents adsorptions conducted with PUF/CNTs/DM/PB; black line represents adsorptions conducted with PUF/DM/PB.

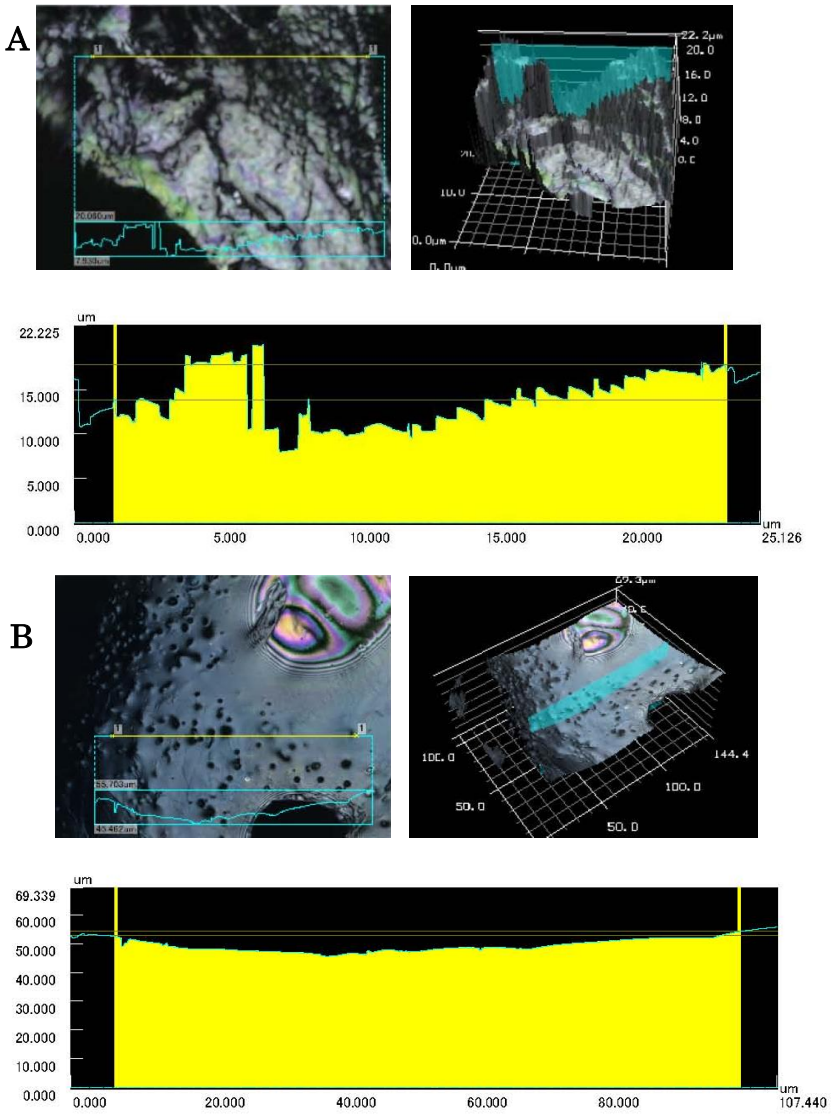

Figure 3-4. Surface roughness of adsorbents with (quaternary) and without (ternary) a CNTs coating. The surface roughness was analyzed in the selected areas (areas boxed in top left panels). (A) The quaternary PUP/CNT/DM/PB adsorbent had a surface roughness of 3.88 ± 0.78um, and (B) the ternary PUP/DM/PB adsorbent had a surface roughness of 3.08 ± 0.23um.

3.3.3 Adsorption isotherms

Adsorption isotherms were plotted to evaluate the PUF/CNTs/DM/PB adsorption of cesium. A Langmuir model was used, because it fit well to the experimental data. The expression of the Langmuir model in this study is:

$$\frac{1}{q_A} = \frac{1}{QK_A}\frac{1}{C_A} + \frac{1}{Q} \quad (1)$$

This was derived from the following Langmuir equation:

$$q_A = \frac{QK_AC_A}{1 + K_AC_A} \quad (2)$$

where q_A is the amount of cesium (mg) absorbed per gram of Prussian blue in the PUP/CNT/DM/PB adsorbent (mg/g); C_A is the equilibrium concentration (mg/L) of cesium in aqueous solution; Q is the theoretical adsorption saturation capacity for a monolayer of the adsorbent (mg/g); and K_A is the Langmuir constant that relates to the affinity of the adsorptive sites (i.e., Prussian blue) for cesium. Figure 3-5 shows a typical adsorption isotherm. The Q value was found to be 166.67 mg/g, which was

comparable or better than the Q value (158.47 mg/g) obtained from the Langmuir isotherm plotted from adsorption data with Prussian blue alone as the adsorbent. In other words, after immobilizing Prussian blue in the spongiform matrix with our caging approach in diatomite and coating with highly dispersed CNTs, its function improved for adsorbing cesium. The linear coefficient (R^2) of the Langmuir isotherm exceeded 0.99; this suggested that the PUF/CNTs/DM/PB adsorbed cesium according to the Langmuir adsorption model. Adsorption isomers were also plotted with the q_A as a function of the amount of cesium absorbed per gram of spongiform matrix (i.e., the overall weight of the quaternary PUF/CNTs/DM/PB adsorbent). This showed that the quaternary spongiform matrix that contained 1.79 wt% Prussian blue had a Q value of 2.94 mg/g. In other words, one gram of the PUF/CNTs/DM/PB-1.79% adsorbent was capable of adsorbing 2.94 mg of cesium. K_A, the Langmuir constant, was found to be 0.8814 for PUF/DM/PB, and 0.8841 for PUF/CNTs/DM/PB, indicating a fact that Prussian blue is the essential adsorptive sites for cesium.

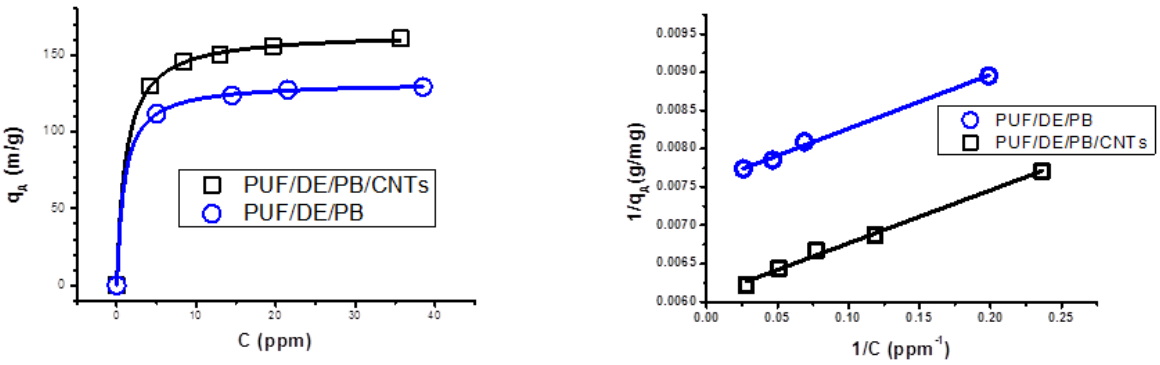

Figure 3-5 Langmuir isotherms for cesium-133 adsorption by the PUF/CNTs/DM/PB and PUF/DM/PB adsorbents; temperature was maintained at 25 ℃ during the experiments.

3.3.4 Elimination efficiency

The elimination efficiency of the quaternary spongiform adsorbent was evaluated as a function of the amount added (mg); Figure 3-6 summarizes the experimental data. Different amounts of PUF/CNTs/DM/PB-1.79% adsorbent were tested at an initial nonradioactive cesium-133 concentration of 10.0 ppm. Cesium-133 was eliminated with an efficiency of 95.96% by adding 0.3 g of PUF/CNTs/DM/PB-1.79% adsorbent to 40 mL of the 10.0 ppm cesium-133 solution. Similar results were also observed for the samples prepared by dissolving cesium-133 in seawater. This result indicated that the Prussian blue based spongiform adsorbents were an excellent and highly selective for the cesium ions.

3.3.5 Mechanism of adsorption

The PUF/CNTs/DM/PB adsorbent takes up cesium ions from the aqueous solution based on ion-exchange. We analyzed the amount of absorbed cesium and the amount of released sodium (Figure 3-7). Cesium ions were exchanged for sodium ions almost stoichiometrically. Prussian blue is a cubic, lattice-based, crystal with ferrous and ferric atoms occupying alternate corners of the cubic lattice, and cyanide groups on the edges (J.F. Keggin, 1936). The alkali atoms, which are exchangeable with cesium ions, are located at the centers of alternating cubes. Among the alkali ions, cesium ion has the highest affinity for occupying the centers of these alternating cubes of Prussian blue. The charge density played the key role with the relationship of activity. It is generally appreciated that the ionic radius of the hydrated ions were followed by $Li^+<Na^+<K^+<Cs^+$, this indicated that the behaviors of charge to size ratio would reduce if under the ions with the similar charges from lithium ion to cesium ion. Therefore, lithium ion showed the least capability of ion exchange, while cesium was considered as the most favorite for the sodium/potassium ions exchange within the alternating cubes of Prussian blue. (Akadémiai Kiadó, 2010). In another words, among the

alkali metal ions, cesium ions was being the largest but with the same charge, this phenomenon resulted the cesium ions possessing low charge density and capable of ionic binding with the exchanger. At the same time, the exchange of sodium and/or potassium for cesium is nearly irreversible. This unique affinity of cesium for Prussian blue confers a high selectivity and a high elimination efficiency for removing radioactive cesium from saline water, like seawater and body fluids.

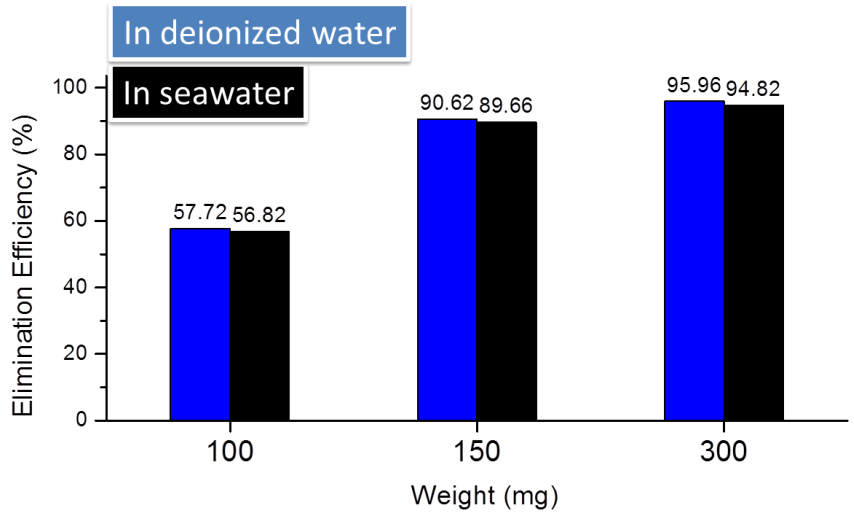

Figure 3-6. Cesium elimination efficiency as a function of the amount (mg) of spongiform adsorbent, PUF/CNTs/DM/PB-1.79%. Samples were tested in 40 ml aqueous solutions containing 10.0 ppm cesium. (10 hours for each sample). Blue column: The elimination efficiency for the sample prepared by dissolving cesium nitrate in deionized water. Black column: Represent of the samples prepared by dissolving cesium nitrate in seawater.

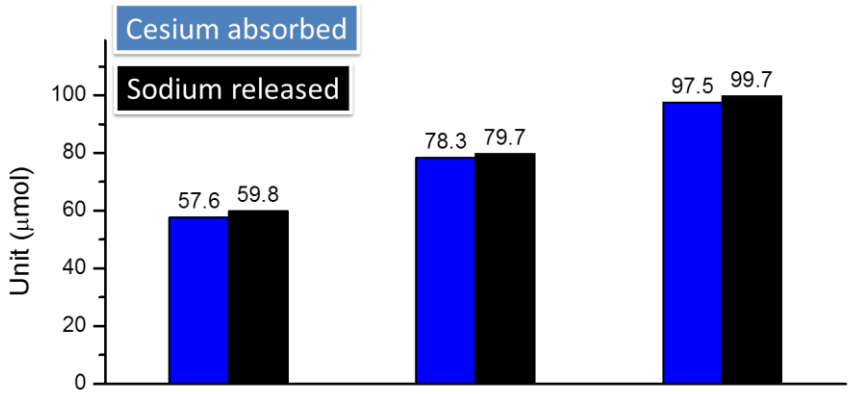

Figure 3-7. Cesium uptake by the PUF/CNTs/DM/PB-1.79% adsorbent and the amount of released sodium ions.

3.3.6 Elimination of radioactive cesium-137

Simulated radioactive water samples were prepared by adding cesium-137 into deionized water and seawater. We chose a cesium-137 activity of 1.50 Bq/ml (4.66 x 10^{-7} ppm). The simulated water samples (10 ml) were taken up into the spongiform absorbents (approximately 0.25 g of each adsorbent). After about 10-hours of water/spongy contacting, the water was squeezed from the spongiform adsorbents and the residual radioactivity in the water was analyzed. The Prussian blue based spongiform adsorbent gave promising results in their practical applications. Figure 3-8 showed that the elimination efficiency for cesium-137 was 99.93% in deionized water and 99.47% in seawater, respectively; indicating the high selectivity and the high capacity for the adsorption of radioactive cesium-137. Additionally, we can observed that after creating the CNTs-network on the surface of the diatomite/Prussian blue composite and fabricating with Polyurethane, the elimination ratio have been increased 11.26% in deionized water and 17.47% in seawater, respectively. This indicated that the enhancement of adsorption capability was caused by CNTs. It is possible for CNTs to assist the cesium ion adsorption in the Prussian blue crystal lattices through charge transfer, this

available charge-transfer was provided by CNTs conjugated **π**-electrons interacted with surrounding substances (Shuji TsuruoKa, 2013). Previous study demonstrated that the grapheme oxide (GO) was a suitable material for decontamination of nuclear waste solution than other routinely used adsorbents such as bentonite clays and activated carbon (AC) in the simulated nuclear waste solutions (Romanchuk, Slesarev, Kalmykov, Kosynkin, and Tour, 2013), this phenomena indicating that the graphene plane with curvature in the structure of CNTs caused nuclear waste sorption. In this study, more interaction details between cesium ions and the surface of CNTs was the motivation of the further studies.

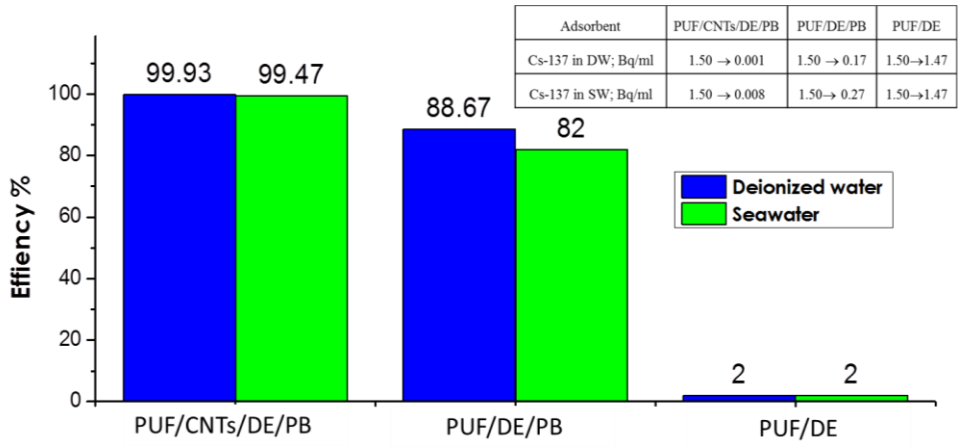

Figure 3-8. Radioactive cesium-137 in simulated samples, before and after adsorption. Each 10.0 ml of deionized water (DW) or seawater (SW) contained cesium-137 (initial radioactivity, 1.50 Bq/ml) sample was taken up (absorbed) with 250 mg of PUF/CNTs/DM/PB, PUF/DM/PB, or the polyurethane polymer combined with diatomite (PUF/DM). *The elimination efficiency was calculated from the initial (C_0) and final (C) cesium-137 concentrations: $(C_0\text{-}C)/C_0\times100\%$.

3.4 Conclusion

We have developed high-performance spongiform adsorbents through fabrication of the spongiform adsorbents with the CNTs-network/diatomite/Prussian-blue as the functioning elements. The resultant ternary (CNTs-network/diatomite/Prussian-blue) composites were mixed with polyurethane pre-polymers to produce the spongiform adsorbents through an in situ foaming procedure. The CNTs-network/diatomite/Prussian-blue composites have been permanently immobilized into the cell-walls of the polyurethane foam. Macro-sized, durable, and flexible spongiform adsorbent was established. Cesium-133 was used for studying the adsorptive capabilities of the Prussian-blue based spongiform absorbent and the caged Prussian blue showed a theoretical capacity of 167mg/g for cesium, indicating a fact that the Prussian blue based spongiform is an excellent adsorbent for the adsorbent of cesium. Carbon nanotubes were able to seal in Prussian blue particles and they enhanced the adsorption of cesium. Adsorption isotherms plotted based on Langmuir equation gave liner line, suggesting that the caged Prussian blue adsorbed cesium in the Langmuir adsorption manner. Cesium was absorbed primarily

by ion-exchange mechanism. For evaluating the practical application of our spongiform adsorbent, deionized water and seawater, each containing 1.50 Bq cesium-137 were decontaminated with the spongiform adsorbent. The elimination efficiency was found to be 99.93% for the deionized water sample and 99.47% for the seawater sample, respectively; indicating the high selectivity and the high capacity for the adsorption of radioactive cesium-137. The studies on the adsorptive behaviors showed that low-levels of radioactive cesium could be selectively eliminated from water with the spongiform adsorbent that incorporated Prussian blue as the functional moiety. In addition, it is worth to mention that the cesium elimination with our spongiform adsorbent was accomplished by self-uptake of the radioactive species from the aqueous solution.

3.5 References

Akadémiai Kiadó, c.-p. w. S. S. B. M. B. V., Formerly Kluwer Academic Publishers B.V. (2010). Lithium, rubidium and cesium ion removal using potassium iron(III) hexacyanoferrate(II) supported on polymethylmethacrylate. *Journal of Radioanalytical and Nuclear Chemistry* 288, 79-88.

Deng, R., Davies, P., and Bajaj, A. K. (2003). Flexible polyurethane foam modelling and identification of viscoelastic parameters for automotive seating applications. *Journal of Sound and Vibration* 262, 391-417.

El-Shahat, M. F., Moawed, E. A., and Burham, N. (2008). Preparation, characterization and applications of novel iminodiacetic polyurethane foam (IDA-PUF) for determination and removal of some alkali metal ions from water. *Journal of Hazardous Materials* 160, 629-633.

J.F. Keggin, F. D. M. (1936). Structures and formula of the Prussian blues and related compounds. *Nature* 4 577-578.

Lefebvre, J., Bastin, B., Le Bras, M., Duquesne, S., Paleja, R., and Delobel, R. (2005). Thermal stability and fire properties of conventional flexible polyurethane foam formulations. *Polymer Degradation and Stability* 88,

28-34.

Lemos, V. A., Santos, M. S., Santos, E. S., Santos, M. J. S., dos Santos, W. N. L., Souza, A. S., de Jesus, D. S., das Virgens, C. F., Carvalho, M. S., Oleszczuk, N., Vale, M. G. R., Welz, B., and Ferreira, S. L. C. (2007). Application of polyurethane foam as a sorbent for trace metal pre-concentration — A review. *Spectrochimica Acta Part B: Atomic Spectroscopy* 62, 4-12.

Li, S., Li, C., Li, C., Yan, M., Wu, Y., Cao, J., and He, S. (2013). Fabrication of nano-crystalline cellulose with phosphoric acid and its full application in a modified polyurethane foam. *Polymer Degradation and Stability* 98, 1940-1944.

M. Khodakovskaya, E. D., M. Mahmood, Y. Xu, Z. Li, F. Watanabe, A.S. Biris, . (2009). Carbon nanotubes are able to penetrate plant seed coat and dramatically affect seed germination and plant growth. *ACS Nano* 3, 3221-3227.

Moawed, E. A., and El-Shahat, M. F. (2013). Synthesis, characterization of low density polyhydroxy polyurethane foam and its application for separation and determination of gold in water and ores samples. *Analytica Chimica Acta*

788, 200-207.

Neng, N. R., Pinto, M. L., Pires, J., Marcos, P. M., and Nogueira, J. M. F. (2007). Development, optimisation and application of polyurethane foams as new polymeric phases for stir bar sorptive extraction. *Journal of Chromatography A* 1171, 8-14.

Osmanlioglu, A. E. (2007). Natural diatomite process for removal of radioactivity from liquid waste. *Applied Radiation and Isotopes* 65, 17-20.

Rein, G., Lautenberger, C., Fernandez-Pello, A. C., Torero, J. L., and Urban, D. L. (2006). Application of genetic algorithms and thermogravimetry to determine the kinetics of polyurethane foam in smoldering combustion. *Combustion and Flame* 146, 95-108.

Romanchuk, A. Y., Slesarev, A. S., Kalmykov, S. N., Kosynkin, D. V., and Tour, J. M. (2013). Graphene oxide for effective radionuclide removal. *Physical Chemistry Chemical Physics* 15, 2321-2327.

Shuji TsuruoKa, B. F., Fitri Khoerunnisa, Daiki Minami (2013). Intensive synergetic Cs adsorbent incorporated with polymer spongiform for scalable purification without post filtration. *Materials Express* 3, 2158-5849.

Xiong, J., Zheng, Z., Qin, X., Li, M., Li, H., and Wang, X. (2006). The

thermal and mechanical properties of a polyurethane/multi-walled carbon nanotube composite. *Carbon* 44, 2701-2707.

Chapter IV

General conclusions

In conclusion, at this study we have demonstrated that low-levels of radioactive cesium could be selectively eliminated from water with spongiform adsorbents that incorporated Prussian blue as the functional moiety. Prussian blue particles were synthesized within the cylindrical cavities of diatomite with an in situ micro-packing approach and sealed in with highly dispersed carbon nanotubes (Chapter 2). Prussian blue particles caged in this manner preferentially absorbed radioactive cesium, despite its permanent immobilization on the cell walls of polyurethane foam (i.e., the spongiform matrix). Carbon nanotubes were able to seal in Prussian blue particles and they enhanced the adsorption of cesium by binding the surface of diatomite at the same time providing enough mesoporous porosity to induce surface-enriched cesium ions. In addition, after the highly dispersed CNTs was created over the surface of the diatomite/Prussian blue composite and immobilized on the cell walls of the polyurethane form for fabrication the spongiform adsorption (Chapter 3), the material strength had been enhanced. In another words, the dispersed CNTs reinforced the spongiform adsorbents. Furthermore, the adsorbent capability had been enhanced after coating by the highly dispersed CNTs; it is possible for CNTs directly assist the cesium ions

adsorbed in the Prussian blue lattices through charge transfer. This charge transfer was available on account of CNTs have conjugated π-electrons interacted with surrounding substances. Prussian blue played the key role for the cesium ions adsorption in the spongiform adsorbents; it offered rapid and stationary ion exchange in the crystal lattice. Therefore cesium ions were absorbed primarily by ion exchange mechanism. Cesium-133 was used for studying the adsorptive capabilities of the Prussian blue based spongiform adsorbents; langmuir equation model was employed to plot the adsorption isotherms as our data was fitted it well, according to the liner line result, the caged Prussian blue adsorbed cesium ions in the monolayer Langmuir adsorption manner. The theoretical capacity was 167mg/g for cesium ions that the caged Prussian blue revealed; demonstrating that the Prussian blue incorporated spongiform adsorbents is an excellent adsorbent for cesium ions decontamination. Practical application was our ultimate objective, 1.50 Bq/ml radioactive cesium-137 was diluted into 10ml of seawater and deionized water for evaluating the decontamination ability of our Prussian blue based spongiform adsorbents; respectively. After about 10 hours of the water/spongy contacting time, the water was squeezed from the spongy and the residual

radioactivity in the water was analyzed. The elimination efficiency was found to be 99.93% for the deionized water sample and 99.47% for the seawater sample, respectively; indicating the high selectivity and the high capacity for the adsorption of radioactive cesium-137. In addition, it is worth to mention that the cesium elimination with our spongiform adsorbent was accomplished by self-uptake of the radioactive species from the aqueous solution due to the hydrophilic characteristic of the polyurethane composite foam.

It is important to note that another advantage of these spongiform adsorbents is that, after adsorbing radioactive cesium, the adsorbent can be condensed into very small volumes with carbonization. It would be considered as one of the promising adsorbents used in the separation of practical application and reprocessing of nuclear wastes. This provides a desirable, practical approach for reducing the final volumes of radioactive waste. Currently, our research groups have used this spongiform, Prussian blue-based adsorbent for the elimination of radioactive cesium from low-level radioactive water in Fukushima areas, and preliminary results have been highly satisfactory. For the actual *in-situ* applications, the ratio of water/spongiform-adsorbent was chosen at 1/1 (volume/volume); after the

radioactive cesium being adsorbed, the water was squeezed from the adsorbent using machine arms. All these achievements obtained in this study are highly beneficial to environmental remediation.

Acknowledgements

Writing of this dissertation has become one of the most significant academic challenges that I have ever had to face. I wouldn’t able to complete this dissertation without the support, patience and guidance help from my supervisor, friends, and my beloved family. It is to them that I owe my deepest gratitude.

I am sincerely appreciated to my supervisor: Professor Bunshi Fugetsu, for his dedicated guidance, and thoughtful ideals throughout the entire process, and for all the things I have learnt from him and for the opportunity to study in his laboratory. I would never been able to finish my work and dissertation without his help. I really enjoyed the life since arrived in Japan. I am very appreciated to Professor Hideyuki Hisashi and Professor Fumio Watari; who were always willing to help and provided best suggestions. Special thanks also go to all academic brothers and sisters in my group.

Likewise, I would like to thank Professor Hongwen Yu for always having answers to my questions, no matter whether scientific or from daily life. I am also grateful to my colleagues from the division of environmental science and those who used to study in my lab, especially to Doc. Sun Ling and Mrs.

Sugawara for pushing me go ahead all the time. My greatest appreciation and friendship goes to my closest friend, Doc. Yu Le, who was always a great support in all my struggles and frustrations in my life and studies.

Finally, I would like to thank my beloved family, for always supporting me, encouraging me, cheering me up and stood by me through the bad and good times.